Glycoconjugate Journal (1991) **8**:456–483

Data bank of three-dimensional structures of disaccharides: Part II, *N*-acetyllactosaminic type N-glycans. Comparison with the crystal structure of a biantennary octasaccharide

ANNE IMBERTY[1]*, MARIE-MADELEINE DELAGE[2], YVES BOURNE[3], CHRISTIAN CAMBILLAU[3] and SERGE PÉREZ[2]

[1] *Laboratoire de Synthèse Organique, Faculté des Sciences, 2 rue de la Houssinière, F-44072 Nantes cédex 03, France*

[2] *Laboratoire de Physicochimie des Macromolécules, INRA, BP 527, F-44026 Nantes cédex 03, France*

[3] *Laboratoire de Cristallographie et de Cristallisation des Macromolécules Biologiques, Faculté de Médecine Secteur Nord, F-13326 Marseille cédex 15, France*

Received 13 March 1991, revised 20 June 1991

Conformational energy maps and descriptions of structures at the local minima are presented for the following fragments found in *N*-acetyllactosaminic type glycans of N-glycoproteins: GlcNAcβ(1-2)Man, GlcNAcβ(1-4)Man, GlcNAcβ(1-6)Man, Galβ(1-4)GlcNAc, GlcNAcβ(1-3)Gal, Fucα(1-6)GlcNAc, Fucα(1-3)GlcNAc, Xylβ(1-2)Man, Galβ(1-3)GlcNAc and GlcNAcβ(1-6)Gal. These results are the second part of a data bank on glycoprotein moieties; five disaccharides found in oligomannose type N-glycans were analysed earlier (Imberty *et al.*, 1990, *Glycoconjugate J* **7**:27–54). In the present study, three to seven minima are found for each dimer. Conformations of disaccharide fragments found in the crystal structure of the complex of a biantennary octasaccharide with *Lathyrus ochrus* lectin are plotted on these energy maps. While the observed conformations are at predicted minima, they are not always at the minimum predicted to have the lowest energy. Further, not all observed conformations are stabilized by the exo-anomeric effect. We conclude that these oligosaccharides are highly flexible.

Keywords: oligosaccharide, three-dimensional structure, modeling, *Lathyrus ochrus* lectin.

Abbreviations: LOL1, *Lathyrus ochrus* isolectin I.

The data bank presented here contains the three-dimensional structures of disaccharide fragments which constitute the glycan moiety of N-glycoproteins. The rationale for building a body of information on disaccharide conformations was thoroughly presented in the first paper of this series [1]. Briefly, the purpose is to provide a basis for constructing models of larger oligosaccharides. Modelling analyses of disaccharides yield the likely conformations between residues, after an allied effort already gave the details of building blocks, gathered in a data bank of three-dimensional structures of monosaccharides [2]. The previous work, in agreement with another investigation [3], has shown that oligosaccharides should be treated as flexible molecules. Therefore, not only the lowest energy disaccharide conformation, but also the ensemble of possible conformations is presented for each glycosidic linkage in the data bank.

The present work adds analyses of ten disaccharides found in *N*-acetyllactosamine glycans and related oligosaccharides to the five disaccharides of the oligomannose type glycan published earlier [1] (for classification see [4]). The *N*-acetyllactosamine family offers bi- to penta-antennary architectures, some of which are shown in Fig. 1. The inner core can be modified by two substituents: (1) a fucose linked α(1-6) to the innermost *N*-acetylglucosamine residue as in the sugar chains of bovine IgG [5], and (2) a 'bisecting' *N*-acetylglucosamine linked β(1-4) to the mannose residue of the branching point as in the penta-antennary glycan of turtle-dove ovomucoid [6]. An unusual variation is the replacement of a lactosamine disaccharide [Galβ(1-4)GlcNAc] by a β(1-3) linkage between these same two residues

* To whom correspondence should be addressed.

0282-0080/91 $03.00+.12

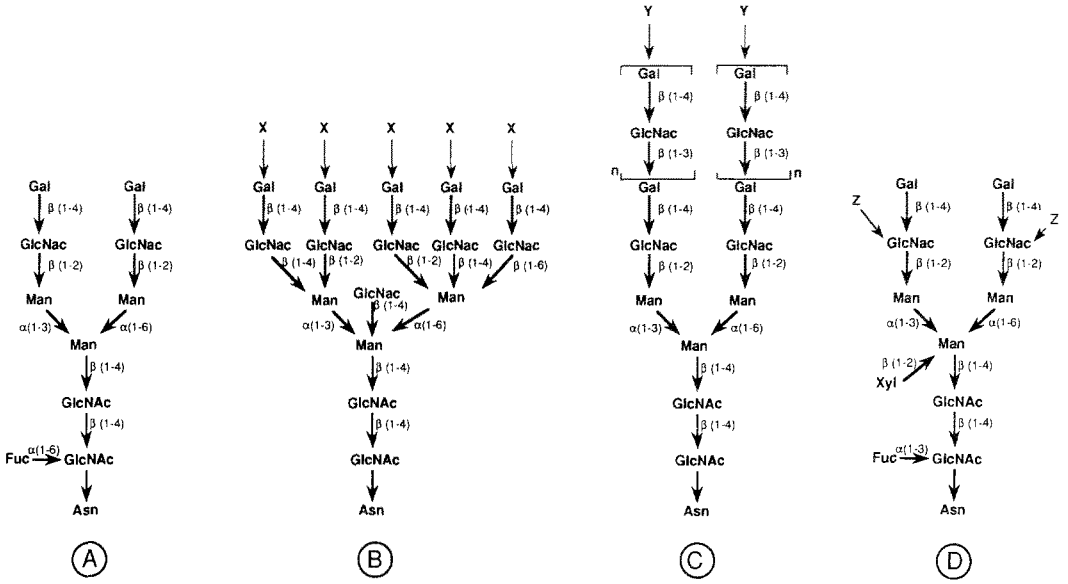

Figure 1. Several examples of *N*-acetyllactosamine type glycans. A, Fucosylated biantennary glycan of bovine IgG [5]; B, bisected penta-antennary glycan of turtle-dove ovomucoid [6] (X being Gal α(1-4)-linked); C, polylactosaminic biantennary glycan of erythrocyte membrane [8] (Y being the blood group determinants); D, example of carbohydrate from plant glycoprotein: glycan from sycamore laccase [11] (Z being Fucα(1-6)-linked).

[7]. More frequently, a polylactosamine sequence occurs. It was first discovered in red cell membrane glycoprotein [8], and is now found in different tumour cell lines [9]. A rare additional branching point, through GlcNAc(1-6)Gal linkages, has been found in the polylactosamine sequence [10].

Besides the *N*-acetyllactosamine family, we include in this paper the plant N-glycans that contain two specific substituents on the common core. A fucose residue can be linked α(1-3) instead α(1-6) to the inner *N*-acetylglucosamine residue, and a xylose residue can be linked β(1-2) to the mannose residue of the branch point, as observed in the carbohydrate chain of sycamore laccase [11]. As shown in Table 1, ten disaccharides have been studied in the present work. The third part of the database, which will include sialylated and other cap disaccharides, is in preparation.

In order to understand how our theoretical analyses might relate to experiment, we compare the torsion angles from the modelling studies with the values found in the crystalline complex of *Lathyrus ochrus* isolectin I (LOL1) with a biantennary octasaccharide [12, 13]. LOL1 is part of a large family of leguminous mannose/glucose specific lectins and has extensive sequence homology with these proteins [14]. Its fine specificity is directed towards a well defined part of biantennary *N*-acetyllactosamine type glycans [15] such as:

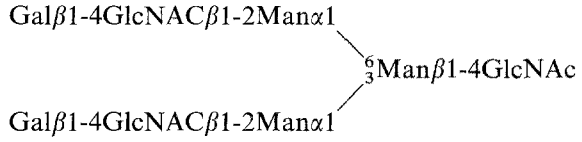

1

Table 1. Disaccharide fragments constituting the *N*-acetyllactosamine type oligosaccharides.

Disaccharide	*Identification in the database*
GlcNAcβ(1-4)GlcNAc[a]	A
Manβ(1-4)GlcNAc[a]	B
Manα(1-3)Man[a]	C
Manα(1-6)Man[a]	E
GlcNAcβ(1-2)Man	F
GlcNAcβ(1-4)Man	G
GlcNAcβ(1-6)Man	H
Galβ(1-4)GlcNAc	I
GlcNAcβ(1-3)Gal	J
Fucα(1-6)GlcNAc	K
Fucα(1-3)GlcNAc	L
Xylβ(1-2)Man	M
GlcNAcβ(1-6)Gal[b]	N
Galβ(1-3)GlcNAc[b]	O

[a] Indicates the disaccharides of the core moiety of N-glycans which have been described in Ref. [1].
[b] Indicates the disaccharide with a very low occurrence which are described in the Appendix.

The crystal structure of the native lectin was recently reported [16] as was the structure of its complex with the trisaccharide Manα(1-3)Manβ(1-4)GlcNAc [17].

Methods

All the model disaccharides studied here were composed of monosaccharides from the database of three-dimensional

structures [2]. Those monosaccharides, derived from crystal structures when available, were optimized with the computer program MM2CARB which contains a force-field appropriate to the carbohydrate field [18].

Nomenclature

In all the following examples, the primed atoms belong to the reducing residue. The two torsion angles describing a glycosidic linkage can be defined as

$$\Phi = \Theta(\text{O-5—C-1—O-1—C′-X})$$

$$\Psi = \Theta(\text{C-1—O-1—C′-X—C′-X} + 1)$$

which corresponds to the crystallographic nomenclature; or as

$$\Phi_H = \Theta(\text{H-1—C-1—O-1—C′-X})$$

$$\Psi_H = \Theta(\text{C-1—O-1—C′-X—H′-X})$$

which correspond to the NMR nomenclature. The primary hydroxyl group orientation of each residue is defined as

$$\chi = \Theta(\text{O-6—C-6—C-5—O–5})$$

or

$$\chi_H = \Theta(\text{O-6—C-6—C-5—H-5}).$$

This corresponds also to the third torsion angle of an α(1-6) linkage ω,

$$\omega = \Theta(\text{O-1—C′-6—C′-5—O′-5})$$

or

$$\omega_H = \Theta(\text{O-1—C′-6—C′-5—H′-5}).$$

The conformations of the χ and ω torsion angles are referred to as either *gauche-trans* (GT) (χ or $\omega = 60°$, χ_H or $\omega_H = -60°$), *gauche-gauche* (GG) (χ or $\omega = -60°$, χ_H or $\omega_H = 180°$) and *trans-gauche* (TG) (χ or $\omega = 180°$, χ_H or $\omega_H = 60°$) [19]. In this system, the first word refers to the relationship of O-6 to O-5 and the second word to the relationship of O-6 to C-4. When describing disaccharides, the characteristics of the nonreducing end are stated first. The sign of the torsion angles is defined in agreement with the rules recommended by the IUPAC-IUB Commission of Biochemical Nomenclature [20].

Energy surface calculations

The potential energy surfaces for each disaccharide were computed using the PFOS (potential functions for oligosaccharide structures) program [21]. PFOS evaluates energies for inter-residue van der Waals interactions, torsional rotation and exo-anomeric effects. Hydrogen bonding energies are optional.

The hydroxymethyl group orientation of each residue may be set at any chosen value. For sugars having O-4 in the equatorial configurations (*gluco* configuration), the GG and GT orientations dominate [19, 22], while the GG conformation seldom occurs for *galacto* configuration in which O-4 has an axial configuration [19]. The distribution of conformations for ω in α(1-6) linkages corresponds closely to the orientations of the free hydroxymethyl groups, according to NMR studies for mannobiose [23, 24]. Therefore, energy maps were made with both GG and GT orientations for mannose and *N*-acetylglucosamine, and GT and TG orientations were used for galactose. The glycosidic valence angle of each model disaccharide was given the value of a linkage of the same type as observed in the solid state.

Miscellaneous

All the energy calculations were performed on a Dec MicroVax computer running VMS. The molecular models were drawn using the SYBYL software. Iso-energy maps were made with the MONGO program [25].

Results and discussion

The first eight disaccharides reported here are the building blocks of the *N*-acetyllactosamine type glycans and are lettered in continuity with the first part of the database [1]: F, GlcNAcβ(1-2)Man, G, GlcNAcβ(1-4)Man; H, GlcNAcβ-(1-6)Man; I, Galβ(1-4)GlcNAc; J, GlcNAcβ(1-3)Gal; K, Fucα(1-6)GlcNAc. Two of them are specific to the plant N-glycans: L, Fucα(1-3)GlcNAc; and M, Xylβ(1-2)Man. Two disaccharides with a very low occurrence in N-glycans (i.e., N, GlcNAcβ(1-6)Gal and O, Galβ(1-3)GlcNAc) have been studied but are presented only as supplementary material (Tables A1, A2, Figs A11–A13) in the Appendix.

The data bank

For each of the disaccharides, the data bank contains the potential energy surfaces and a detailed description of the conformations at the local minima. These characteristics are listed in Tables 2–9. The effects from the different O-6 orientations and from the addition of hydrogen bonding are usually minor. Therefore, except for the (1-6) linkages, the maps in Figs 2–6 arise from GT orientations and do not include hydrogen bonding. However, inter-residue hydrogen bonding can be of interest to explain conformational behaviour of a molecule in a particular medium such as a nonpolar solvent or crystalline environment. Therefore, for each local energy minimum a list of possible hydrogen bonds is given in Tables 2–9, and the energy maps including this energy term are presented in the Appendix, Figs A1–A10.

For the ten energy maps displayed in Figs 2–6, the low energy regions, as delineated by the 10 kcal mol^{-1} isoenergy contour, correspond to 10–70% of the total map. Because of the three bonds between the residues, the (1-6) linkages have the largest low-energy areas. Some of the maps have several 'islands' of low energy. The high-energy barriers separating these islands may be artifacts of the rigid residue modelling method [26, 27]. The use of more sophisticated, and more computer time-consuming, molecular mechanics programs demonstrated the existence of low energy pathways which allow the molecule to attain all the

Table 2. Geometrical features, calculated energies (kcal mol^{-1}) and possible hydrogen bonds for the GlcNAcβ(1-2)Man linkage as calculated by the PFOS program ($\tau = 114.5°$). Torsional angles are given in both the crystallography and the NMR nomenclatures, the two sets being presented respectively without and with parentheses.

Name	Φ, Ψ	(Φ_H, Ψ_H)	χ, χ'	(χ_H, χ'_H)	*Relative energy*	*Possible hydrogen bond*
F1	−90, 160	(30, 40)	−60, −60	(180, 180)	0.02	
			60, −60	(−60, 180)	0.00	
			−60, 60	(180, −60)	0.20	
			60, 60	(−60, −60)	0.18	
F2	55, 140	(175, 20)	−60, −60	(180, 180)	1.47	O-7 . . . O-3′ N . . . O-3′
			60, −60	(−60, 180)	1.48	O-7 . . . O-3′ N . . . O-3′
			−60, 60	(180, −60)	1.48	O-7 . . . O-3′ N . . . O-3′
			60, 60	(−60, −60)	1.50	O-7 . . . O-3′ N . . . O-3′
F3	−65, 120	(55, 0)	−60, −60	(180, 180)	1.79	O-5 . . . O-3′
	−60, 120	(60, 0)	60, −60	(−60, 180)	1.75	O-5 . . . O-3′
			−60, 60	(180, −60)	1.84	O-5 . . . O-3′
	−65, 120	(55, 0)	60, 60	(−60, −60)	1.75	O-5 . . . O-3′
F4	85, 175	(−155, 55)	−60, −60	(180, 180)	1.96	
			60, −60	(−60, 180)	2.06	
			−60, 60	(180, −60)	1.99	
			60, 60	(−60, −60)	2.09	
F5	−105, 80	(15, −40)	−60, −60	(180, 180)	2.15	O-5 . . . O-3′
			60, −60	(−60, 180)	2.03	O-5 . . . O-3′
			−60, 60	(180, −60)	2.18	O-5 . . . O-3′
			60, 60	(−60, −60)	2.06	O-5 . . . O-3′

Table 3. Geometrical features, calculated energies (kcal mol^{-1}) and possible hydrogen bonds for the GlcNAcβ(1-4)Man linkage as calculated by the PFOS program ($\tau = 116.4°$). Torsional angles are given in both the crystallography and the NMR nomenclatures, the two sets being presented respectively without and with parentheses.

Name	Φ, Ψ	(Φ_H, Ψ_H)	χ, χ'	(χ_H, χ'_H)	*Relative energy*	*Possible hydrogen bond*
G1	−110, −155	(10, −35)	−60, −60	(180, 180)	0.07	O-5 . . . O-3′
			60, −60	(−60, 180)	0.00	O-5 . . . O-3′
	−115, −155	(5, −35)	−60, 60	(180, −60)	0.19	O-5 . . . O-3′
			60, 60	(−60, −60)	0.13	O-5 . . . O-3′
G2	−70, −110	(50, 10)	−60, −60	(180, 180)	0.58	O-5 . . . O-3′
			60, −60	(−60, 180)	0.53	O-5 . . . O-3′
			−60, 60	(180, −60)	0.69	O-5 . . . O-3′
			60, 60	(−60, −60)	0.64	O-5 . . . O-3′
G3	−100, 50	(20, 170)	−60, −60	(180, 180)	2.16	
			60, −60	(−60, 180)	1.99	
			−60, 60	(180, −60)	2.04	
			60, 60	(−60, −60)	1.83	O-6 . . . O-6′
G4	40, −115	(160, 5)	−60, −60	(180, 180)	2.37	O-7 . . . O-3′ O-6 . . . O-6′
			60, −60	(−60, 180)	2.38	O-7 . . . O-3′ O-6 . . . O-6′
	40, −110	(160, 10)	−60, 60	(180, −60)	2.15	O-7 . . . O-3′
			60, 60	(−60, −60)	2.08	O-7 . . . O-3′
G5	−50, 85	(70, −155)	−60, −60	(180, 180)	6.38	
			60, −60	(−60, 180)	6.11	
			−60, 60	(180, −60)	6.34	
			60, 60	(−60, −60)	6.10	

Table 4. Geometrical features, calculated energies (kcal mol^{-1}) and possible hydrogen bonds for the GlcNAcβ(1-6)Man linkage as calculated by the PFOS program ($\tau = 114.5°$). Torsional angles are given in both the crystallography and the NMR nomenclatures, the two sets being presented respectively without and with parentheses.

Name	Φ, Ψ	(Φ_H, Ψ)	χ, ω'	(χ_H, ω'_H)	*Relative energy*	*Possible hydrogen bond*
Hgg1	−65, −110	(55, −110)	−60, −60	(180, 180)	0.51	
			60, −60	(−60, 180)	0.47	
Hgg2	−65, −175	(55, −175)	−60, −60	(180, 180)	1.15	
			60, −60	(−60, 180)	1.16	
Hgg3	−60, 120	(60, 120)	−60, −60	(180, 180)	1.21	
	−55, 110	(65, 110)	60, −60	(−60, 180)	0.53	
Hgg4	55, 175	(115, 175)	−60, −60	(180, 180)	1.39	
			60, −60	(−60, 180)	1.40	
Hgg5	−125, 95	(−5, 95)	−60, −60	(180, 180)	1.84	
	−130, 95	(−10, 95)	60, −60	(−60, 180)	1.81	
Hgg6	60, −120	(180, −120)	−60, −60	(180, 180)	2.20	O-5 . . . O-4[2] O-6 . . . O-4[5]
			60, −60	(−60, 180)	2.15	O-5 . . . O-4[9] O-6 . . . O-4[5]
Hgt1	−85, −95	(35, −95)	−60, 60	(180, −60)	0.02	
			60, 60	(−60, −60)	0.00	
Hgt2	55, 100	(175, 100)	−60, 60	(180, −60)	0.47	
			60, 60	(−60, −60)	0.50	
Hgt3	−90, 60	(30, 60)	−60, 60	(180, −60)	0.90	
	−90, 65	(30, 65)	60, 60	(−60, −60)	0.80	
Hgt4	−70, 180	(50, 180)	−60, 60	(180, −60)	1.46	
			60, 60	(−60, −60)	1.42	
Hgt5	20, 65	(140, 65)	−60, 60	(180, −60)	1.59	
			60, 60	(−60, −60)	1.74	
Hgt6	70, −170	(−170, −170)	−60, 60	(180, −60)	2.18	
			60, 60	(−60, −60)	2.18	

Table 5. Geometrical features, calculated energies (kcal mol^{-1}) and possible hydrogen bonds for the Galβ(1-4)GlcNAc linkage as calculated by the PFOS program ($\tau = 117.1°$). Torsional angles are given in both the crystallography and the NMR nomenclatures, the two sets being presented respectively without and with parentheses.

Name	Φ, Ψ	(Φ_H, Ψ_H)	χ, χ'	(χ_H, χ'_H)	*Relative energy*	*Possible hydrogen bond*
I1	−75, −105	(45, 15)	60, −60	(−60, 180)	0.00	O-5 . . . O-3′
			180, −60	(60, 180)	0.07	O-5 . . . O-3′
			60, 60	(−60, −60)	0.09	O-5 . . . O-3′
			180, 60	(60, −60)	0.17	O-5 . . . O-3′
I2	−90, 50	(30, 170)	60, −60	(−60, 180)	0.49	O-2 . . . O-3′
			180, −60	(60, 180)	0.74	O-2 . . . O-3′
			60, 60	(−60, −60)	0.39	O-2 . . . O-3′
						O-6 . . . O-6′
			180, 60	(60, −60)	0.68	O-2 . . . O-3′
I3	45, −115	(165, 5)	60, −60	(−60, 180)	0.89	O-2 . . . O-3′
						O-5 . . . O-6′
						O-6 . . . O-6′
	50, −115	(170, 5)	180, −60	(60, 180)	1.06	O-5 . . . O-3′
						O-5 . . . O-6′
	45, −110	(165, 10)	60, 60	(−60, −60)	1.11	O-5 . . . O-3′
			180, 60	(60, −60)	1.32	O-5 . . . O-3′
I4	−130, −150	(−10, −30)	60, −60	(−60, 180)	0.91	O-2 . . . O-6′
			180, −60	(60, 180)	0.95	O-2 . . . O-6′
	−135, −150	(−15, −30)	60, 60	(−60, −60)	1.06	
	−140, −145	(−20, −25)	180, 60	(60, −60)	1.08	
I5	−50, 85	(70, −155)	60, −60	(−60, 180)	3.07	
			180, −60	(60, 180)	3.46	
			60, 60	(−60, −60)	3.03	
			180, 60	(60, −60)	3.43	

Table 6. Geometrical features, calculated energies (kcal mol^{-1}) and possible hydrogen bonds for the GlcNAcβ(1-3)Gal linkage as calculated by the PFOS program ($\tau = 116.0°$). Torsional angles are given in both the crystallography and the NMR nomenclatures, the two sets being presented respectively without and with parentheses.

Name	Φ, Ψ	(Φ_H, Ψ_H)	χ, χ'	(χ_H, χ'_H)	*Relative energy*	*Possible hydrogen bond*
J1	−85, 60	(35, −60)	−60, 60	(180, −60)	0.30	O-5 . . . O-4′
			60, 60	(−60, −60)	0.12	O-5 . . . O-4′
			−60, 180	(180, 60)	0.22	O-5 . . . O-4′
			60, 180	(−60, 60)	0.00	O-5 . . . O-4′
J2	60, 110	(180, −10)	−60, 60	(180, −60)	0.58	O-5 . . . O-2′
			60, 60	(−60, −60)	0.60	O-5 . . . O-2′
	60, 105	(180, −15)	−60, 180	(180, 60)	0.40	O-5 . . . O-2′
			60, 60	(−60, 60)	0.42	O-5 . . . O-2′
J3	−75, 145	(45, 25)	−60, 60	(180, −60)	0.85	
	−80, 140	(40, 25)	60, 60	(−60, −60)	0.81	
			−60, 180	(180, 60)	0.84	
			60, 180	(−60, 60)	0.80	
J4	20, 65	(140, −55)	−60, 60	(180, −60)	1.94	
	25, 60	(145, −60)	60, 60	(−60, −60)	1.95	
	20, 65	(140, −55)	−60, 180	(180, 60)	1.83	
	25, 60	(145, −60)	60, 180	(−60, 60)	1.84	
J5	−35, 170	(85, 50)	−60, 60	(180, −60)	2.14	O-5 . . . O-2′
			60, 60	(−60, −60)	2.00	O-5 . . . O-2′
			−60, 180	(180, 60)	2.13	O-5 . . . O-2′
			60, 180	(−60, 60)	2.00	O-5 . . . O-2′
J6	85, 165	(−155, 45)	−60, 60	(180, −60)	2.51	
			60, 60	(−60, −60)	2.62	
			−60, 180	(180, 60)	2.48	
			60, 180	(−60, 60)	2.59	
J7	−75, −90	(45, 150)	−60, 60	(180, −60)	4.56	O-5 . . . O-2′
			60, 60	(−60, −60)	4.36	O-5 . . . O-2′
						O-6 . . . O-2′
			−60, 180	(180, 60)	4.54	O-5 . . . O-2′
			60, 180	(−60, 60)	4.35	O-5 . . . O-2′
						O-6 . . . O-2′

Table 7. Geometrical features, calculated energies (kcal mol^{-1}) and possible hydrogen bonds for the Fucα(1-6)GlcNAc linkage as calculated by the PFOS program ($\tau = 114.5°$). Torsional angles are given in both the crystallography and the NMR nomenclatures, the two sets being presented respectively without and with parentheses.

Name	Φ, Ψ	(Φ_H, Ψ)	ω′	(ω'_H)	*Relative energy*	*Possible hydrogen bond*
Kgg1	−65, 155	(55, 155)	−60	(180)	0.00	
Kgg2	−110, 80	(10, 80)	−60	(180)	0.38	
Kgg3	−70, −110	(50, −110)	−60	(180)	1.53	
Kgg4	−145, −155	(−25, −155)	−60	(180)	1.71	O-2 . . . O-4′
Kgt1	−95, 65	(25, 65)	60	(−60)	0.23	
Kgt2	−60, 180	(60, 180)	60	(−60)	1.21	
Kgt3	−155, −135	(−35, −135)	60	(−60)	1.65	O-2 . . . O-5′
Kgt4	−70, −100	(50, −100)	60	(−60)	1.79	O-2 . . . O-5′

Table 8. Geometrical features, calculated features, calculated energies (kcal mol^{-1}) and possible hydrogen bonds for the Fucα(1-3)GlcNAc linkage as calculated by the PFOS program ($\tau = 115.0°C$). Torsional angles are given in both the crystallography and the NMR nomenclatures, the two sets being presented respectively without and with parentheses.

Name	Φ, Ψ	(Φ_H, Ψ_H)	χ′	(χ'_H)	*Relative energy*	*Possible hydrogen bond*
L1	−70, 145	(50, 25)	−60	(180)	0.00	O-2 . . . O-7′ O-5 . . . O-4′
			60	(−60)	0.01	O-2 . . . O-7′ O-5 . . . O-4′
L2	−145, 95	(25, −25)	−60	(180)	0.71	O-5 . . . N′
			60	(−60)	0.71	O-5 . . . N′
L3	−100, 80	(20, −40)	−60	(180)	1.66	O-5 . . . O-4′
			60	(−60)	1.68	O-5 . . . O-4′

Table 9. Geometrical features, calculated energies (kcal mol^{-1}) and possible hydrogen bonds for the Xylβ(1-2)Man linkage as calculated by the PFOS program ($\tau = 116.5°$). Torsional angles are given in both the crystallography and the NMR nomenclatures, the two sets being presented respectively without and with parentheses.

Name	Φ, Ψ	(Φ_H, Ψ_H)	χ′	(χ'_H)	*Relative energy*	*Possible hydrogen bond*
M1	−65, 110	(55, −10)	−60	(180)	0.00	O-5 . . . O-3′
			60	(−60)	0.01	O-5 . . . O-3′
M2	−105, 75	(15, −45)	−60	(180)	0.70	O-5 . . . O-3′
			60	(−60)	0.70	O-5 . . . O-3′
M3	45, 115	(165, −5)	−60	(180)	1.46	O-2 . . . O-3′
	35, 120	(155, 0)	60	(−60)	1.48	O-2 . . . O-3′

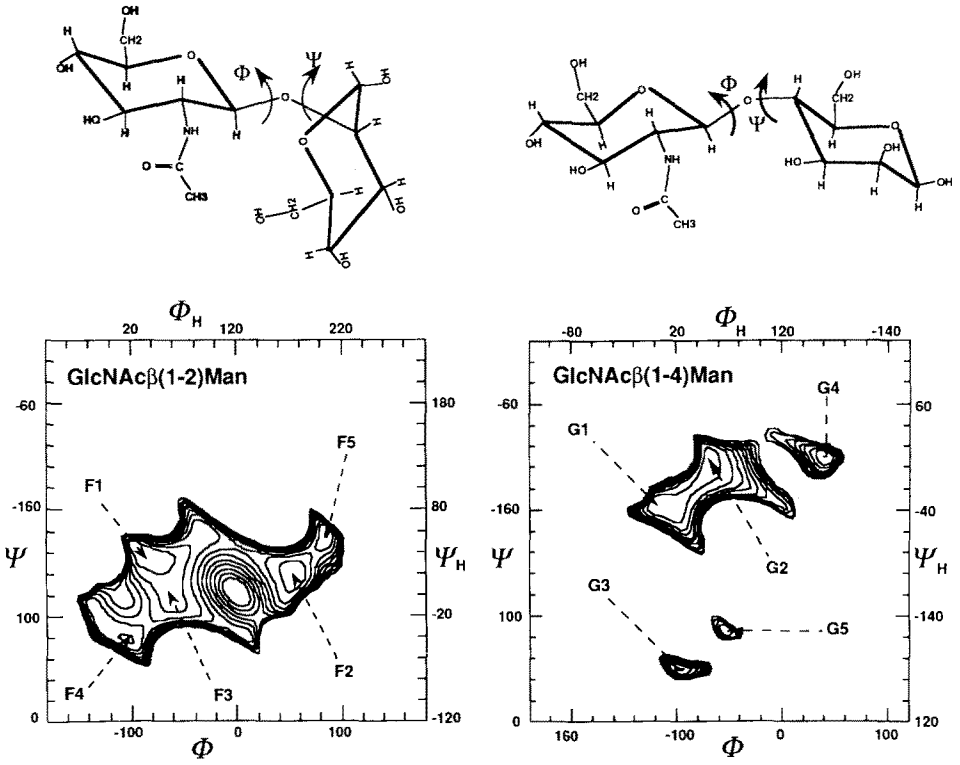

Figure 2. Iso-energy maps of the GlcNAcβ(1-2)Man and GlcNAcβ(1-4)Man disaccharides as a function of the Φ and Ψ torsion angles. The hydroxymethyl groups are fixed in a GT orientation. Iso-energy contours are drawn by interpolation of 1 kcal mol^{-1} with respect to the absolute minima F1 and G1. All the energy minima are located on the surfaces and numbered by increasing energy. The labelling of the axes at the bottom and the top are different since they correspond to the crystallographic and NMR nomenclature (see the Methods section), respectively. The same convention is used for left and right axes.

conformational states. As a consequence, none of these isolated minima should be ignored when modelling oligosaccharides.

It is often assumed that the ideal conformation of an oligomer has standard residue geometries, with each linkage at the minimum energy conformation. The assumption of linkage independent appears to have a number of exceptions, especially for these N-glycan structures. Branching points, (1-2) linkages and interactions between antennae all provide conditions that may favour minima other than the one with lowest energy for an isolated disaccharide. Experimental evidence has been obtained from NMR data that the solution behaviour of a disaccharide can be substantially modified when included in a complex multiantennary oligomer [28]. Therefore, as described earlier [1], it is necessary to optimize the whole oligosaccharide structure.

Description of the crystal structure of LOL1-complex with the models

The crystal structure of the complex between the biantennary *N*-acetyllactosamine octasaccharide and the *Lathyrus ochrus* lectin has been solved to 2.3 Å [13] and refined by X-PLOR [29] to an R factor of 0.19, with RMS deviations from ideal bond lengths and angles of 0.01 Å and 3.1 deg, respectively. The data presented here are the ones from crystallographic refinement, without further energy minimization. Nevertheless, it has been checked that energy refinement will yield only slight deviations from crystal structure.

In the complex, all the sugar rings are in the expected $^4C_1$ conformation. The mannose residue of the (1-3) lactosamine arm is buried in the recognition site of the lectin. In addition to this specific interaction, the (1-6) arm is interacting with the protein surface through numerous van der Waals interactions. The molecular basis of the interaction between the protein and the sugar will be discussed elsewhere and we will focus here only on the structural features of the glycan which yield new data about oligosaccharide conformation. Figure 7 shows the glycan in the crystal conformation, along with the energy maps for the linkages. The conformations in the crystal are shown on the corresponding maps and their characteristics are listed in Table 10. The maps for Manβ(1-4)GlcNAc, Manα(1-3)Man and Manα(1-6)Man are from the first part of this series [1].

Only the number 5 linkage in the octamer has the same conformation as the lowest energy model. All the other octamer linkages correspond to higher energy local minima. In particular, the Manα(1-3)Man and the Manβ(1-4)GlcNAc linkages are trapped in conformations far from the main low energy wells. Previously, it was suggested that these

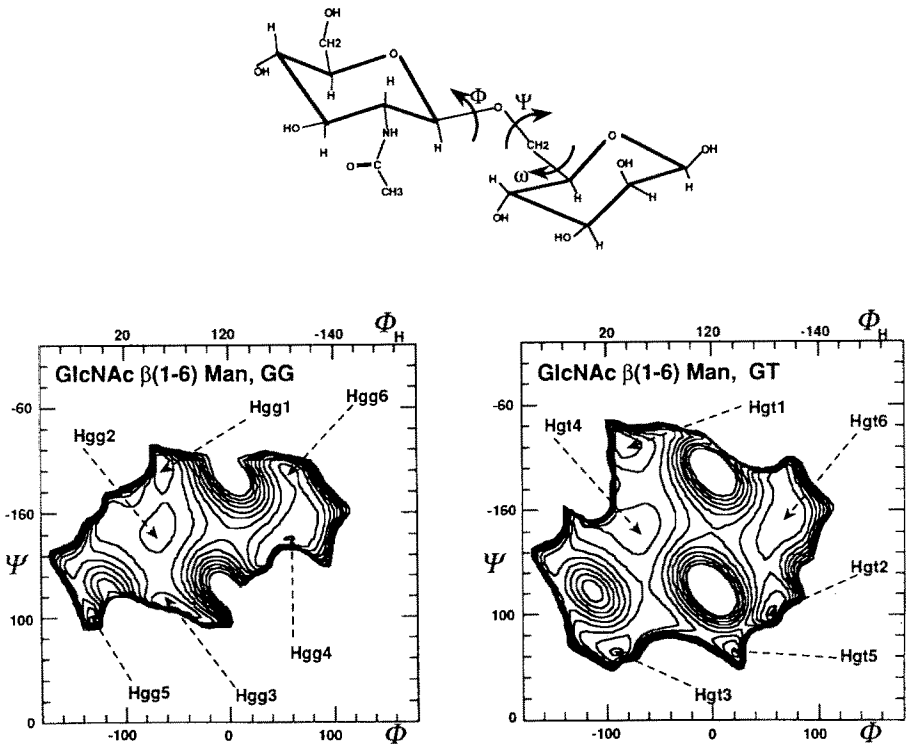

Figure 3. Iso-energy maps of the GlcNAcβ(1-6)Man disaccharide as a function of the Φ and Ψ torsion angles. The third torsion angle of the linkage is fixed in the GG orientation ($\omega = -60°$, $\omega_H = 180°$) in the left panel and in the GT orientation ($\omega = +60°$, $\omega_H = -60°$) in the right panel. Other details are as in Fig. 2, the minima being labelled from Hgg1 to Hgg6 and from Hgt1 to Hgt6.

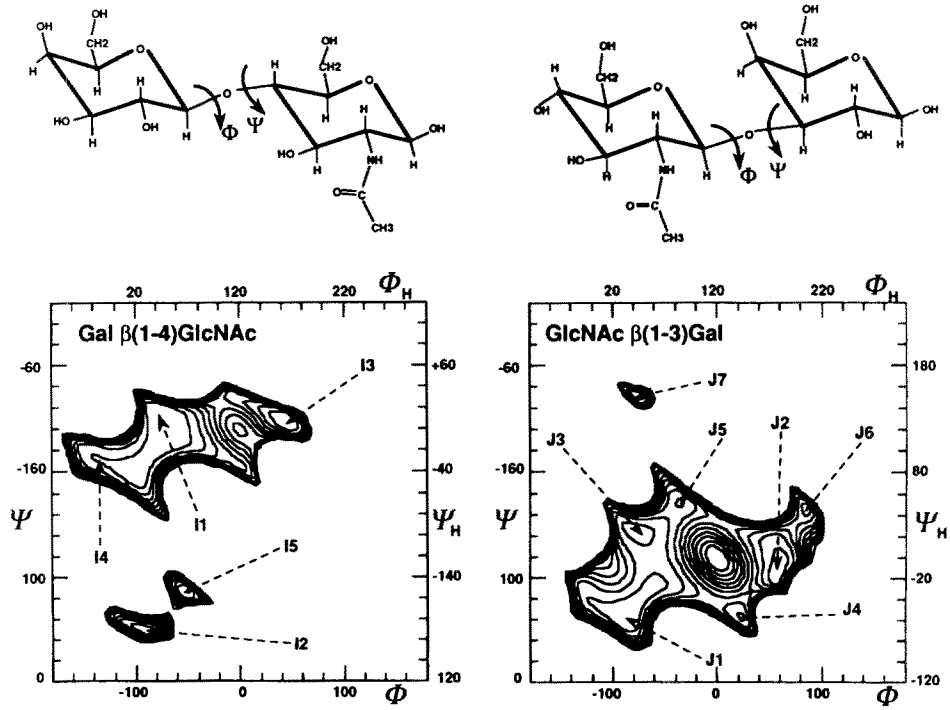

Figure 4. Iso-energy maps of the Galβ(1-4)GlcNAc and GlcNAcβ(1-3)Gal disaccharides as a function of the Φ and Ψ torsion angles. Other details are as in Fig. 2, the energy minima being labelled from I1 to I5 and from J1 to J7.

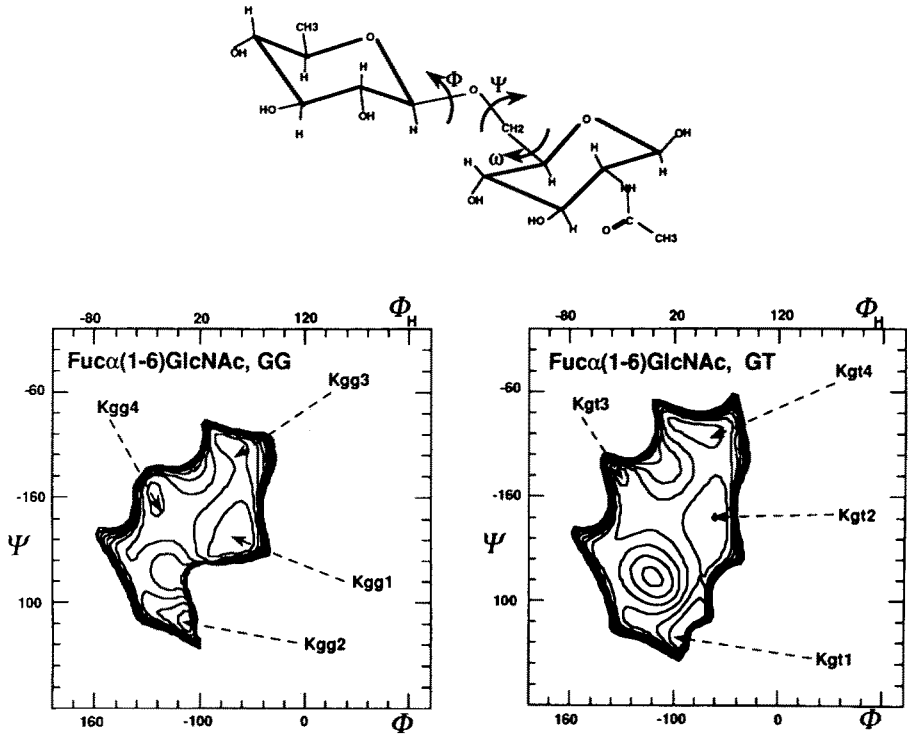

Figure 5. Iso-energy maps of the Fucα(1-6)GlcNAc disaccharide as a function of the Φ and Ψ torsion angles. The third torsion angle of the linkage is fixed in the GG orientation ($\omega = -60°$, $\omega_H = 180°$) in the left panel and in the GT orientation ($\omega = +60°$, $\omega_H = -60°$) in the right panel. Other details are as in Fig. 2, the minima being labelled from Kgg1 to Kgg4 and from Kgt1 to Kgt6.

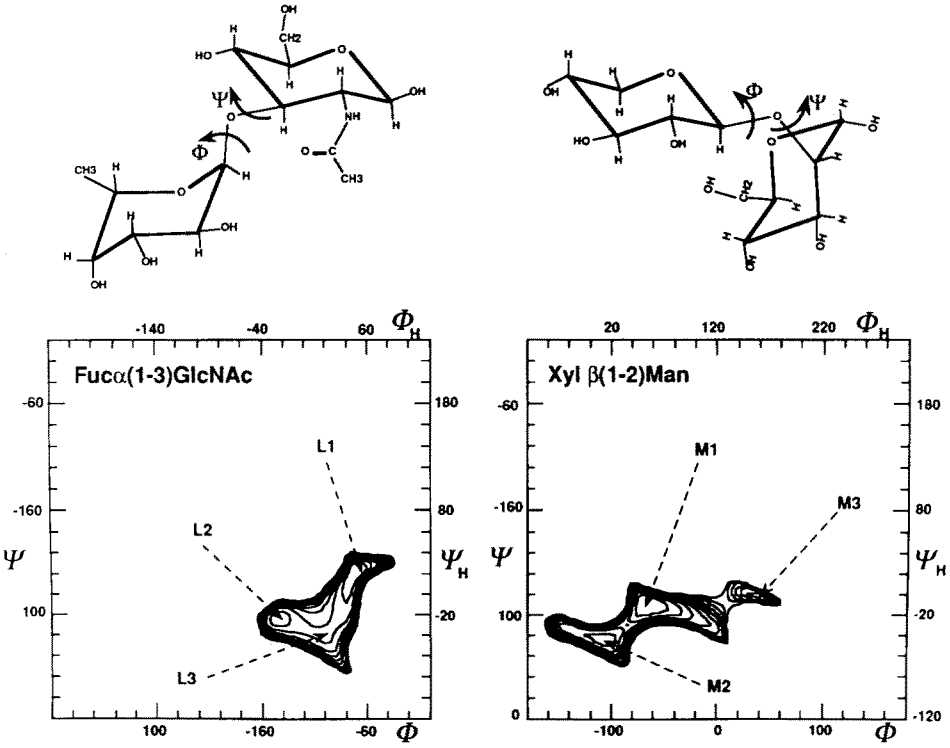

Figure 6. Iso-energy maps of the Fucα(1-3)GlcNAc and Xylβ(1-2)Man disaccharides as a function of the Φ and Ψ torsion angles. Other details are as in Fig. 2, the energy minima being labelled from L1 to L3 and from M1 to M3.

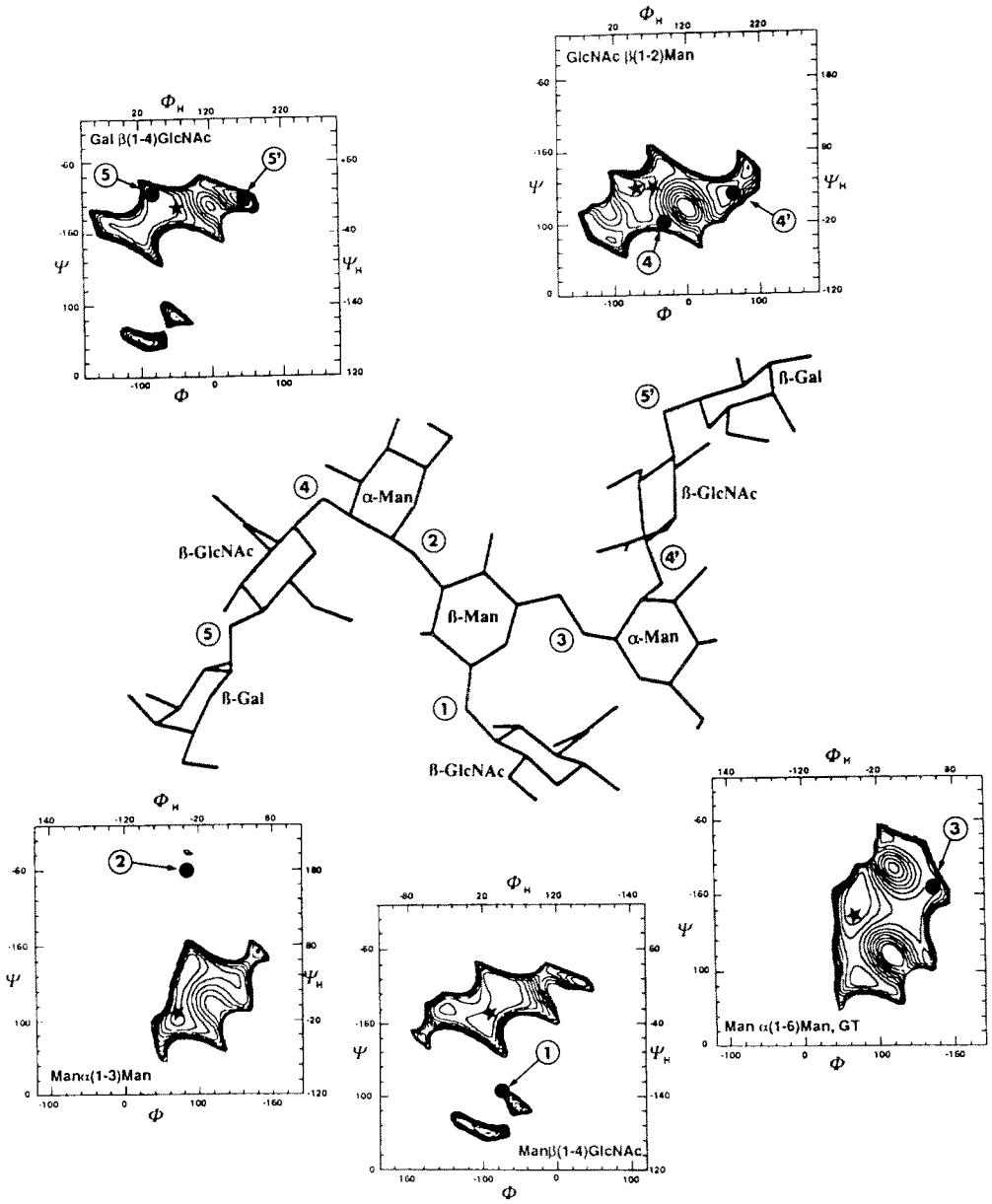

Figure 7. Graphic representation of the biantennary octasaccharide as observed in the crystal of the lectin/sugar complex. Each linkage has been numbered and the conformation, indicated by a dot, reported on the corresponding Φ, Ψ map extracted from the database. For comparison, the linkages conformations of the glycan of human IgG_1 have been indicated by an * in the corresponding energy maps (torsion angles values from Ref. [38]).

remote wells could be occupied [30]. This structure adds evidence from a cellobiose structure [31] showing that remote alternative minimum can be occupied. For the Manα(1-6)Man linkage, Φ is about 120° from the conformation most stabilized by the exo-anomeric effect. Linkages 4′ and 5′ would be stabilized even less by the exo-anomeric effect. This shows that the exo-anomeric effect does not, by itself, determine oligosaccharide conformations and should not be overestimated.

The flexibility of N-acetyllactosaminic glycans

Some of the energy maps presented here can be compared with previous modelling studies. The GlcNAcβ(1-6)Man linkage has been investigated by Cumming and Carver [32] in an original way, the energy being calculated as a function of the three torsion angles Φ, Ψ and ω. Potential energy surfaces of Xylβ(1-2)Man and Fucα(1-3)GlcNAc linkages of plant glycoproteins reported recently [33] exhibit a very limited accessible domain with only one low energy conformation. From the conformational maps of this work (Fig. 6), these two linkages are not among the most flexible ones, but both of them can reach three low energy conformations. Such discrepancies arise from the use of different potential function for the energy calculations. The previous investigations were conducted with the widely used

Table 10. Geometrical characteristics of all the linkages of the bi-antennary octosaccharide as measured by x-ray diffraction.

Linkage	*Number (Fig. 7)*	Φ *(deg)*	Ψ *(deg)*	ω *(deg)*	*Corresponding conformation*
Manβ(1-4)GlcNAc	1	−74	106		B6
Manα(1-3)Man	2	90	−74		C6
Manα(1-6)Man	3	177	−134	GT	Egt3
GlcNAcβ(1-2)Man	4	73	152		F3
	4′	−38	101		F2
Galβ(1-4)GlcNAc	5	−95	−104		I1
	5′	39	−102		I3

HSEA program [34], which contains too large a weighting for the exo-anomeric effect, leading to a drastic shrinkage of the potential map about the Φ axis [18].

Since the first CPK model of a biantennary glycan [35], several structures have been proposed, based on the combination of conformational analysis and NMR experiments [36, 37] and most of them have been recently reviewed [38]. These similar models all had rigid linkages with conformations corresponding to the lowest energy on the respective maps. The only predicted flexibility was at the α(1-6) linkage, where the ω torsion angle was thought to take both the GG and GT orientations.

Besides the LOL1/octasaccharide complex described herein, the only solid state information about N-glycans arose from the crystal structure of a glycoprotein, the Fc fragment of human immunoglobulin IgG_1 [39]. The conformation of the complex type decasaccharide has been extensively described in recent reviews [38, 40]. The conformations of the glycosidic bonds have been reported in the energy maps of Fig. 7 and it appears that each linkage conformation corresponds to the energy minimum. Comparison has been made [40] between the crystalline conformation of the glycan [39] and its solution conformation in aqueous solution, as inferred from high resolution NMR spectroscopy and force field calculations [37]. The two conformations were reported to be almost similar, except for the Ψ angle of the Manα(1-6)Man linkage. This variation was interpreted to result from interactions occurring between the (1-6) lactosamine arm and the surface of the protein.

One might, from these earlier works, conclude that biantennary lactosamine glycans are essentially rigid, with flexibility located only at the α(1-6) linkage. However, the conformational maps in this study and the unambiguous diffraction evidence from the LOL1/glycan complex give a different conclusion. These molecules have a variety of available conformations and can adopt arrangements that correspond to higher-energy local minima in response to local conditions. The slight increase in internal potential energy can be compensated by van der Waals and hydrogen bonding interactions. Further, the alternative minima are sufficiently close in energy and the barriers between them are sufficiently low that a number of these minima will be significantly populated in solution. Such conclusions are in agreement with a previous modelling study that proposed several low energy conformations for biantennary glycans [41]. On the other hand, some other oligosaccharides, such as blood group determinants, have been demonstrated to have very limited internal motions [42].

From a methodological point of view, this example provides a perfect illustration that it is essential not to restrict a conformational study to the search for the lowest or so-called 'global' energy minimum. Oligosaccharides are flexible and they can adopt many conformations within the low energy domains. Furthermore, all these other conformations can be of importance when further stabilizing energy is provided by the interaction with a partner.

Acknowledgements

Part of this work was supported by the French Ministère de la Recherche et de l'Enseignement Supérieur, Grant n° MRES87 T O 261.

References

1. Imberty A, Gerber S, Tran V, Pérez S (1990) *Glycoconjugate J* 7:27–54.
2. Pérez S, Delage MM (1991) *Carbohydr Res* **212**:253–9.
3. Carver JP, Mandel D, Michnick SW, Imberty A, Bradye JW (1990) In *Computer Modeling of Carbohydrate Molecules, ACS Symposium Series 430* (French AD, Brady JW, eds) pp. 266–80. Washington DC: American Chemical Society.
4. Montreuil J (1980) *Adv Carbohydr Chem Biochem* **37**:157–223.
5. Fujii T, Nishiura T, Nishikawa A, Miura R, Taniguchi N (1990) *J Biol Chem* **265**:6009–18.
6. François-Gérard C, Brocteur J, Andre A, Gerday C, Pierce-Cretel A, Montreuil J, Spik G (1980) *Blood Transf Immunohaem* **XXII**:579–87.
7. Mizuochi T, Taniguchi T, Fujikawa K, Titani K, Kobata A (1983) *J Biol Chem* **258**:6020–24.

8. Krusius T, Finne J, Rauvala H (1978) *Eur J Biochem* **92**:289–300.
9. Yamamoto K, Tsuji T, Tarutani O, Osawa T (1984) *Eur J Biochem* **143**:133–44.
10. Fukuda M, Dell A, Fukuda MN (1984) *J Biol Chem* **259**:4782–91.
11. Takahashi N, Hotta T, Ishihara H, Mori M, Tejima S, Bligny R, Akazawa T, Endo S, Arata Y (1986) *Biochemistry* **25**:388–95.
12. Bourne Y, Anguille C, Fontecilla-Camps JC, Rougé P, Cambillau C (1990) *J Biol Chem* **213**:211–13.
13. Bourne Y, Rougé P, Cambillau C (1991) *J Biol Chem* (in press).
14. Rougé P, Borrebaeck CAK, Richardson M, Yarwood A (1987) *Glycoconjugate J* **4**:371–8.
15. Debray H, Rougé P (1984) *FEBS Lett* **176**:120–4.
16. Bourne Y, Abergel C, Cambillau C, Frey M, Rougé P, Fontecilla-Camps JC (1990) *J Mol Biol* **214**:571–84.
17. Bourne Y, Rougé P. Cambillau C (1990) *J Biol Chem* **265**:18161–65.
18. Tvaroska I, Pérez S (1986) *Carbohydr Res* **149**:389–410.
19. Marchessault RH, Pérez S (1979) *Biopolymers* **18**:2369–74.
20. IUPAC-IUB Commission on Biochemical Nomenclature (1971) *Arch Biochem Biophys* **145**:405–21.
21. Pérez S (1978) DSc Thesis, University of Grenoble, France.
22. Nishida Y, Ohrui H, Meguro H (1984) *Tetrahedron Lett* **25**:1575–78.
23. Cumming DA, Carver JP (1987) *Biochemistry* **26**:6676–83.
24. Hori H, Nishida Y, Ohrui H, Meguro H, Uzawa J (1988) *Tetrahedron Lett* **29**:4457–60.
25. Pogge R, MONGO Program, Lick Observatory, CA, USA. Vax Graphic Station version by Tom Lew, University of Toronto, Canada.
26. Tran V, Buléon A, Imberty A, Pérez S (1989) *Biopolymers* **28**:679–90.
27. Imberty A, Pérez S, Tran V (1989) *J Comp Chem* **11**:206–16.
28. Cumming DA, Shah RN, Krepinsky JJ, Grey AA, Carver JP (1987) *Biochemistry* **26**:6655–63.
29. Brünger AT, Kuriyan J, Karplus M (1987) *Science* **235**:458–60.
30. Pérez S, Vergelati C (1987) *Polymer Bull* **17**:141–8.
31. Bock K, Meyer B, Thiem J (1978) *Angew Chem Int Ed Engl* **17**:447–9.
32. Cumming DA, Carver JP (1987) *Biochemistry* **26**:6664–76.
33. Bouwstra JB, Spoelstra EC, de Waard, P, Leeflang BR, Kamerling JP, Vliegenthart JFG (1990) *Eur J Biochem* **190**:113–22.
34. Thogersen H, Lemieux RU, Bock K, Meyer B (1982) *Can J Chem* **60**:44–57.
35. Strecker G, Montreuil J (1979) *Biochimie* **61**:1199–246.
36. Brisson JR, Carver JP (1983) *Can J Biochem Cell Biol* **61**:1067–78.
37. Paulsen H, Peters T, Sinnwell V, Lebuhn R, Meyer B (1985) *Liebigs Ann Chem* 489–509.
38. Meyer B (1990) *Topics Curr Chem* **154**:141–208.
39. Deisenhofer J (1981) *Biochemistry* **20**:2361–70.
40. Paulsen H (1990) *Angew Chem Int Ed Engl* **29**:823–39.
41. Biswas M, Sekharudu YC, Rao VSR (1986) *Int J Biol Macromol* **8**:2–8.
42. Yan Z-Y, Bush CA (1990) *Biopolymers* **29**:799–811.

Appendix

See pages 470–483.

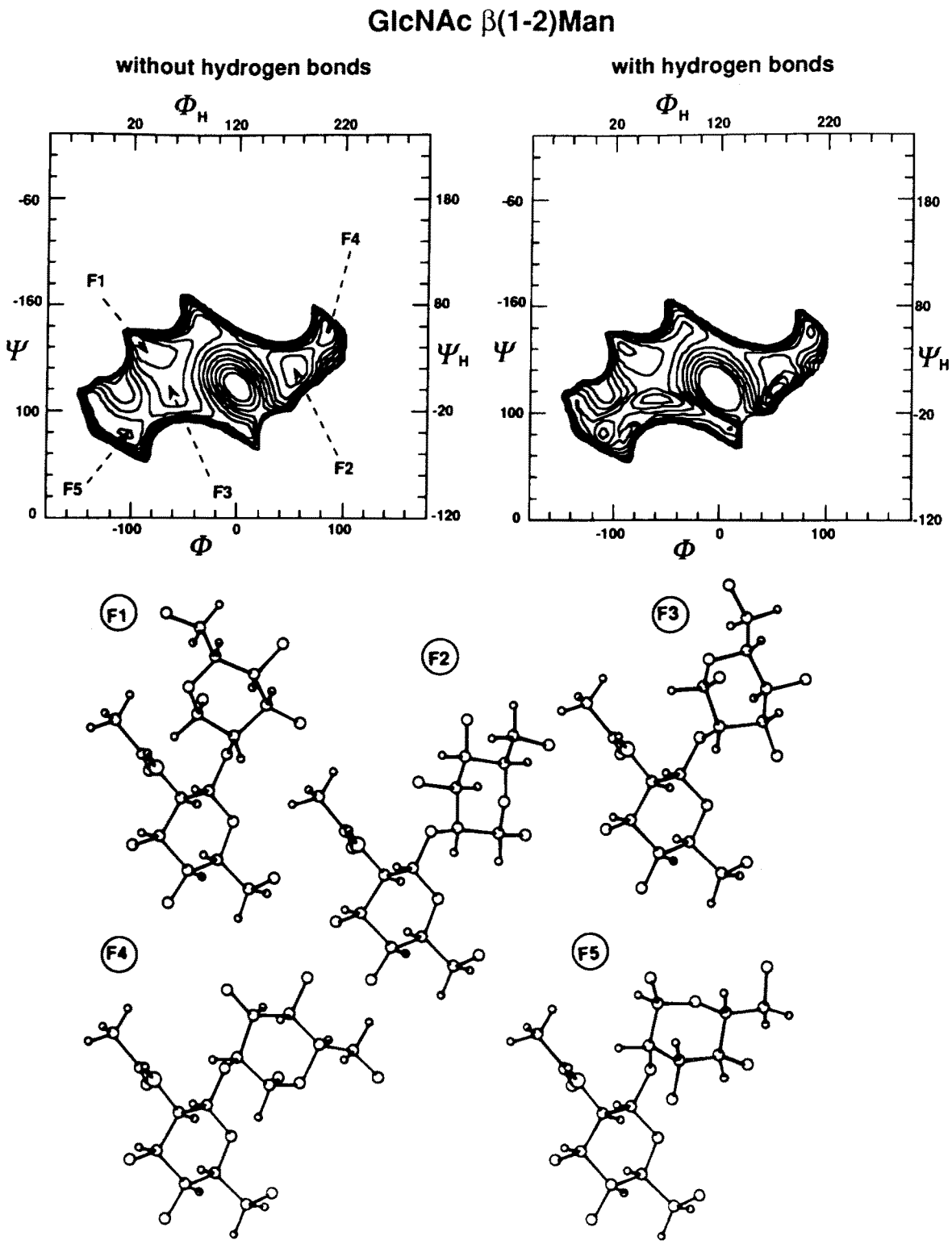

Figure A1. Iso-energy map of the GlcNAcβ(1-2)Man disaccharide as a function of the Φ and Ψ torsion angles. The energy is computed without (left panel) and with (right panel) the contribution arising from hydrogen bonding. The glycosidic valence angle (τ) is fixed at a value of 114.5°. Both hydroxymethyl groups are fixed in a GT orientation. The axes at the bottom and top are differently named since they correspond respectively to crystallography and NMR nomenclature for torsional angles (see the Methods section for nomenclature). The same conventions are used for the left and right axes. Iso-energy contours are drawn by interpolation of 1 kcal mol^{-1} with respect to the absolute minimum (F1). All the energy minima located on the energy map (F1 to F5) are represented by ball and stick drawings (ALCHEMY software, TRIPOS).

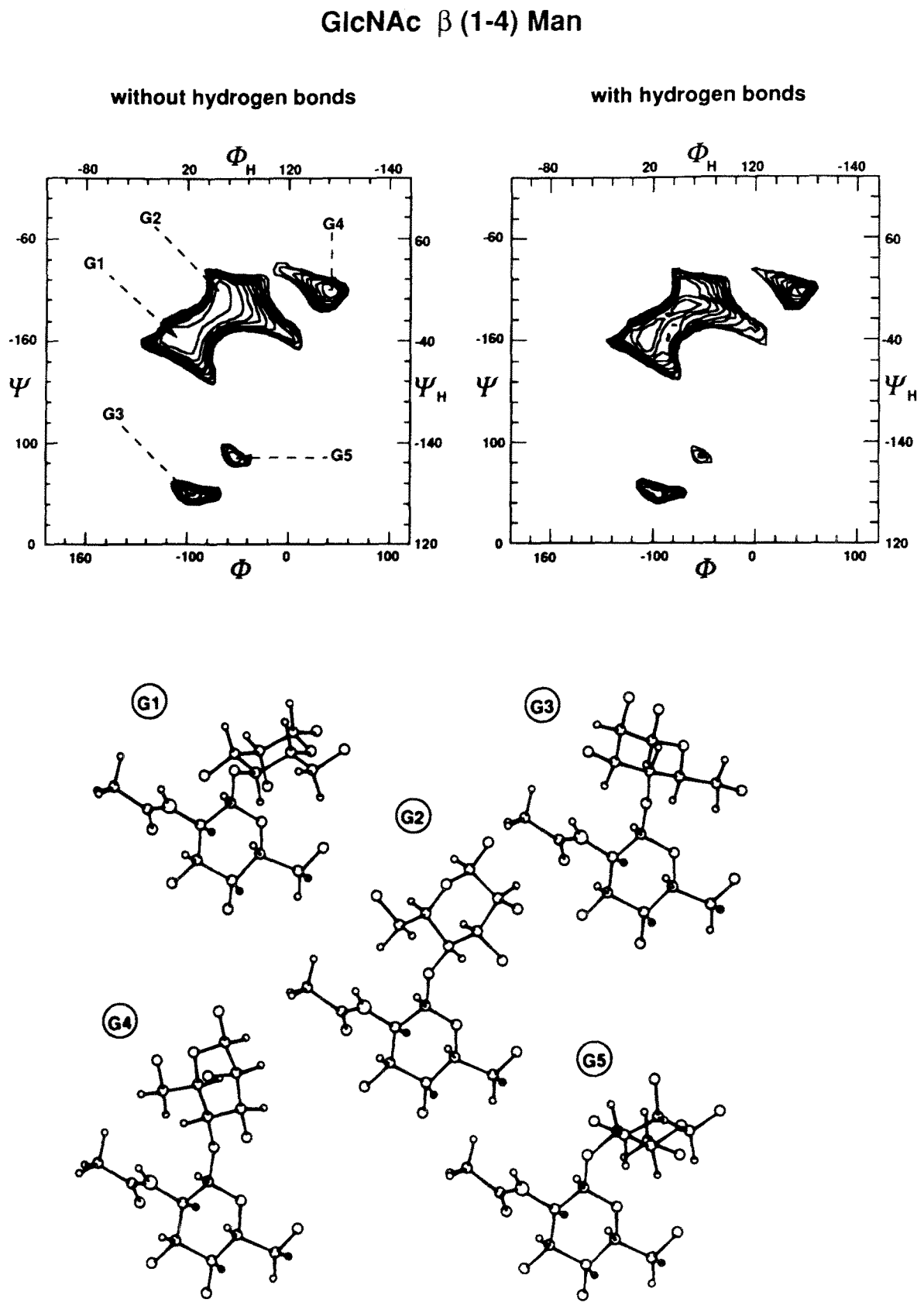

Figure A2. Iso-energy map of the GlcNAcα(1-4)Man disaccharide computed without (left panel) and with (right panel) the contribution arising from hydrogen bonding. The glycosidic valence angle (τ) is fixed at a value of 116.4°. Both hydroxymethyl groups are fixed in a GT orientation. Other details are as in Fig. A1. The drawings represent the energy minima G1 to G5.

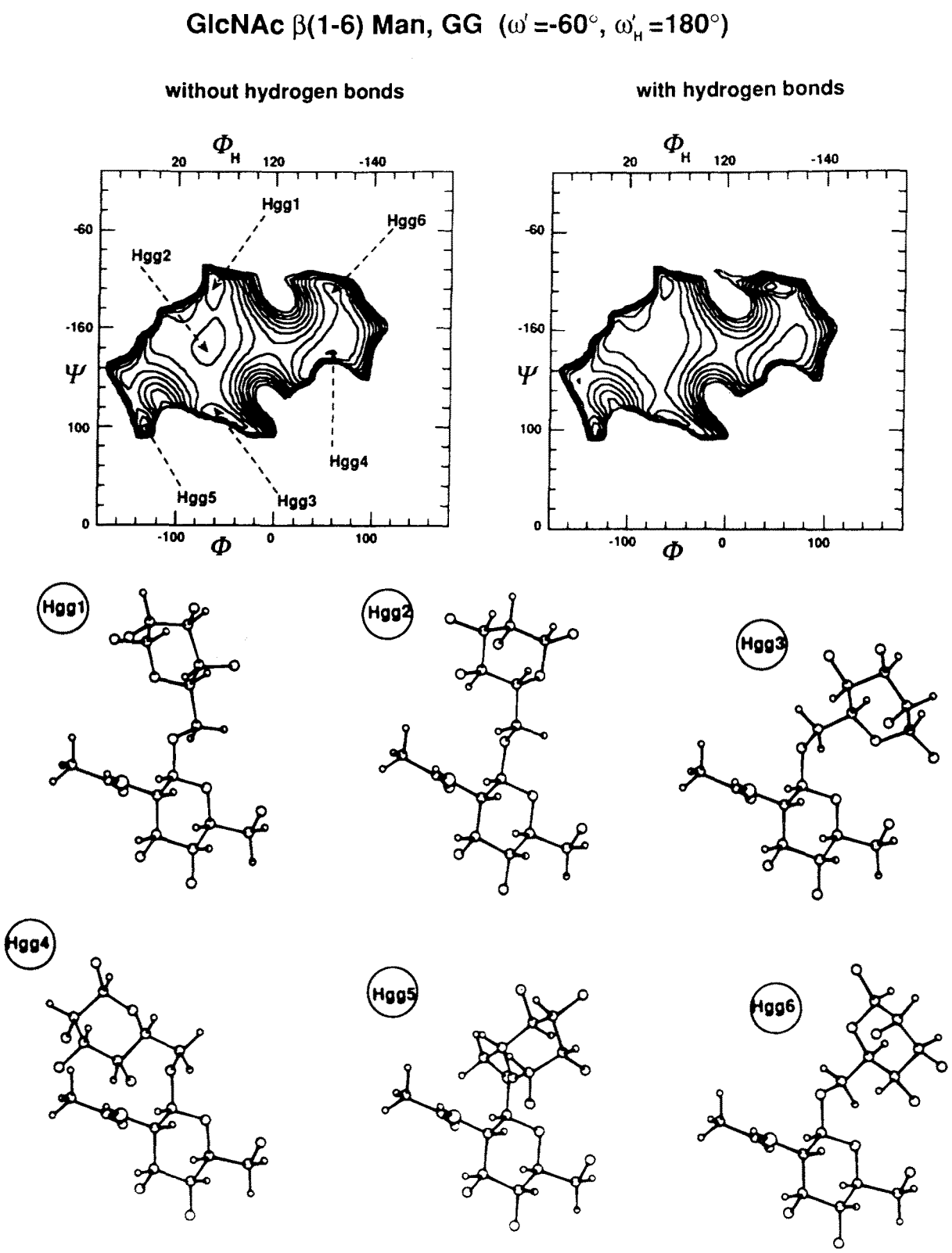

Figure A3. Iso-energy map of the GlcNAcβ(1-6)Man disaccharide computed without (left panel) and with (right panel) the contribution arising from hydrogen bonding. The ω angle at the glycosidic linkage is fixed in the GG orientation whereas the *N*-acetylglucosamine hydroxymethyl group has the GT orientation. The glycosidic valence angle (τ) has a value of 114.5°. Other details are as in Fig. A1. The drawings represent the energy minima Hgg1 to Hgg6.

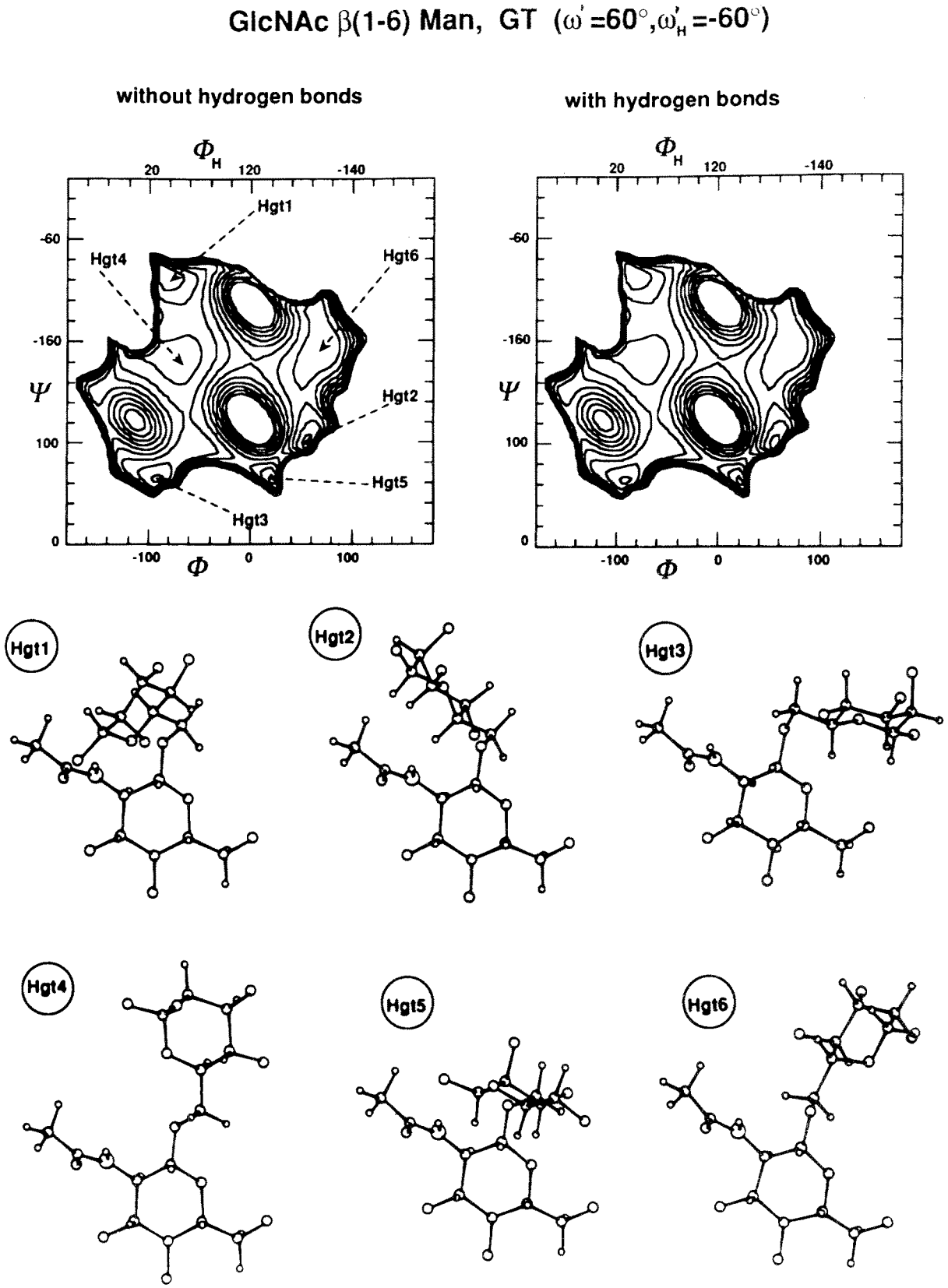

Figure A4. Iso-energy map of the GlcNAcβ(1-6)Man disaccharide computed without (left panel) and with (right panel) the contribution arising from hydrogen bonding. The ω angle at the glycosidic linkage and the *N*-acetylglucosamine hydroxymethol group are fixed in the GT orientation. The glycosidic valence angle (τ) has a value of 114.5°. Other details are as in Fig. A1. The drawings represent the energy minima Hgt1 to Hgt6.

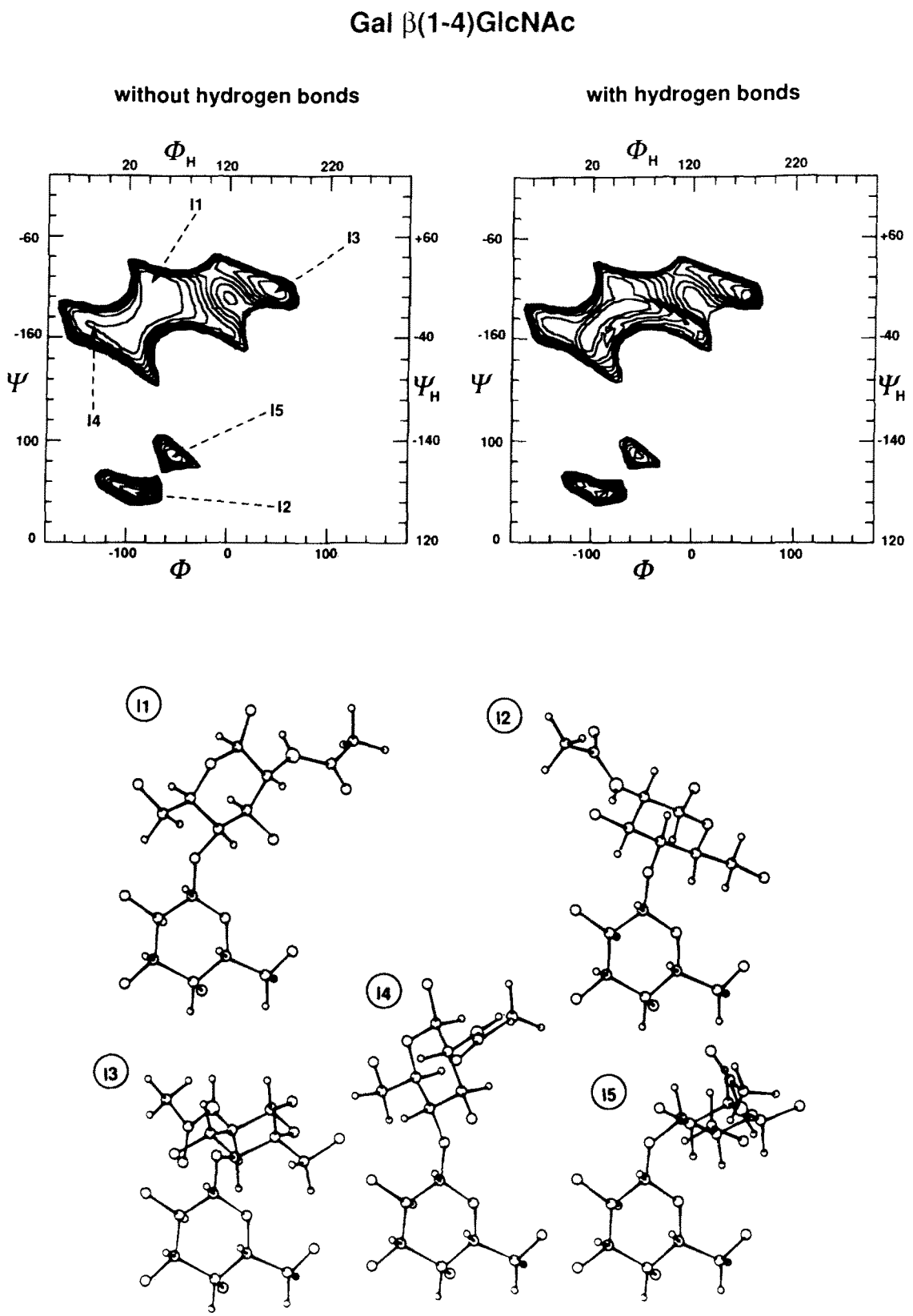

Figure A5. Iso-energy map of the Galβ(1-4)GlcNAc disaccharide computed without (left panel) and with (right panel) the contribution arising from hydrogen bonding. The glycosidic valence angle (τ) is fixed at a value of 117.1°. Both hydroxymethyl groups are fixed in a GT orientation. Other details are as in Fig. A1. The drawings represent the energy minima I1 to I5.

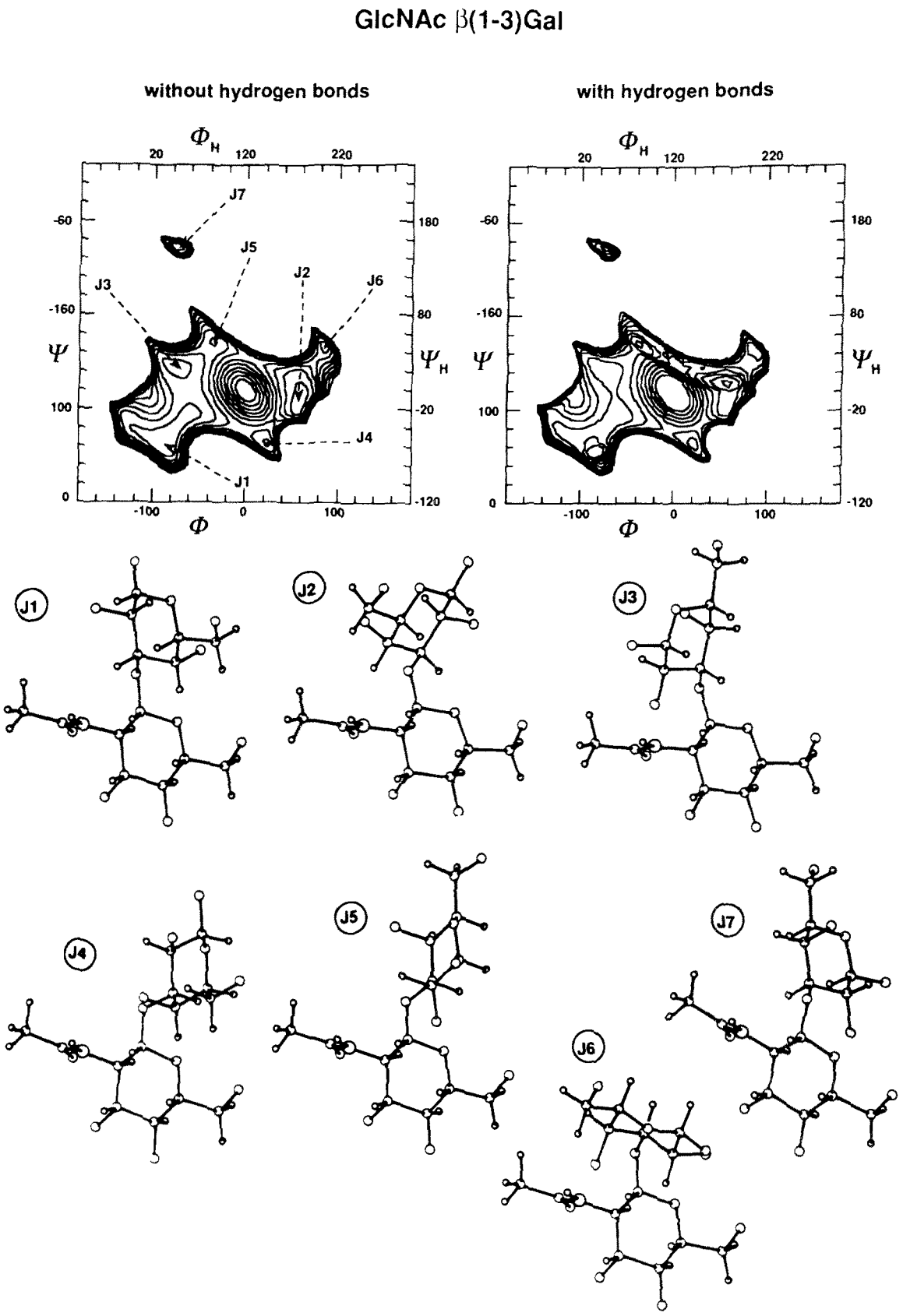

Figure A6. Iso-energy map of the GlcNAcβ(1-3)Gal disaccharide computed without (left panel) and with (right panel) the contribution arising from hydrogen bonding. The glycosidic valence angle (τ) is fixed at a value of 116.0°. Both hydroxymethyl groups are fixed in a GT orientation. Other details are as in Fig A1. The drawings represent the energy minima J1 to J7.

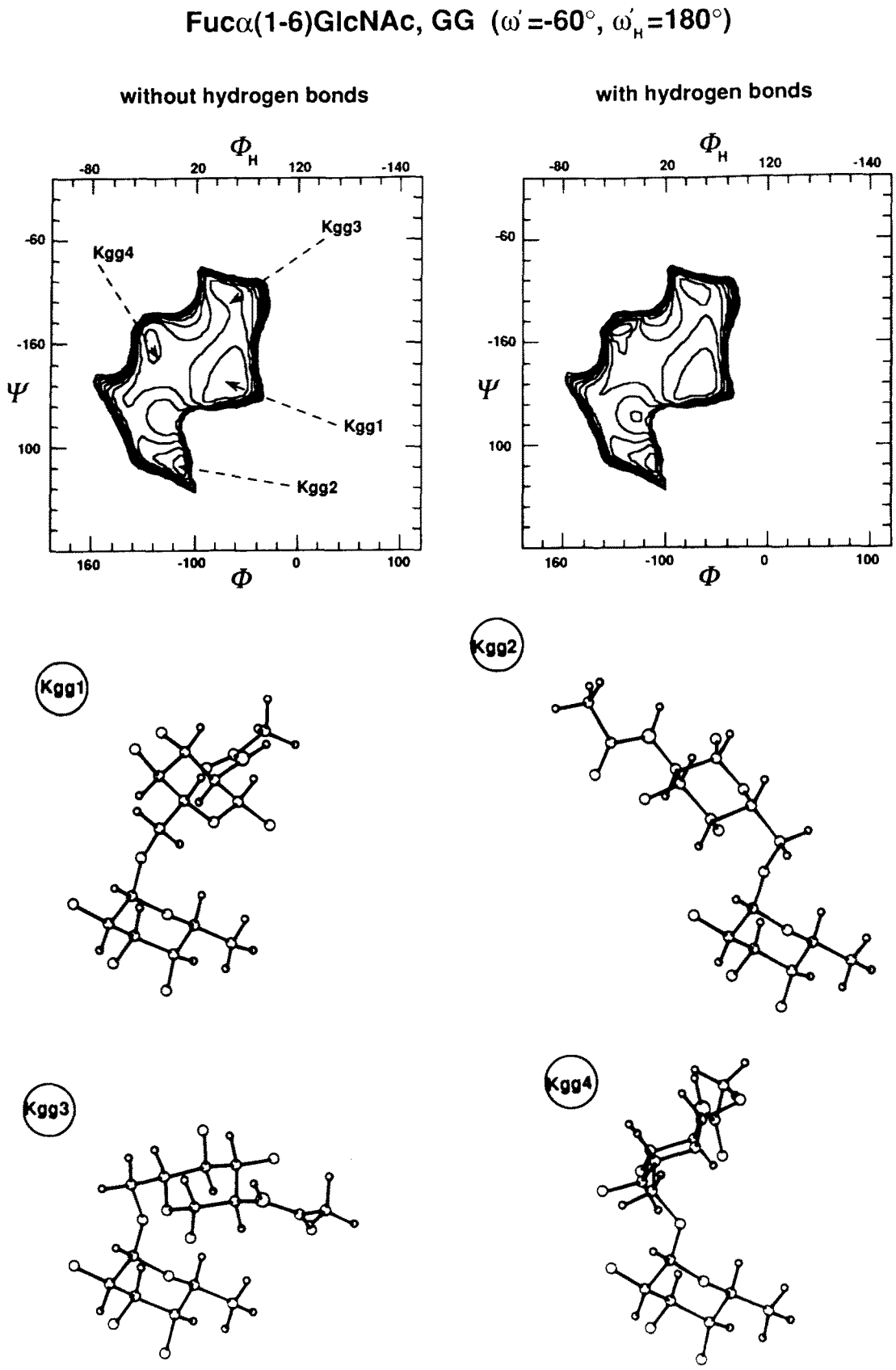

Figure A7. Isoenergy map of the Fucα(1-6)GlcNAc disaccharide computed without (left panel) and with (right panel) the contribution arising from hydrogen bonding. The ω angle at the glycosidic linkage is fixed in the GG orientation. The glycosidic valence angle (τ) has a value of 114.5°. Other details are as in Fig. A1. The drawings represent the energy minima Kgg1 to Kgg4.

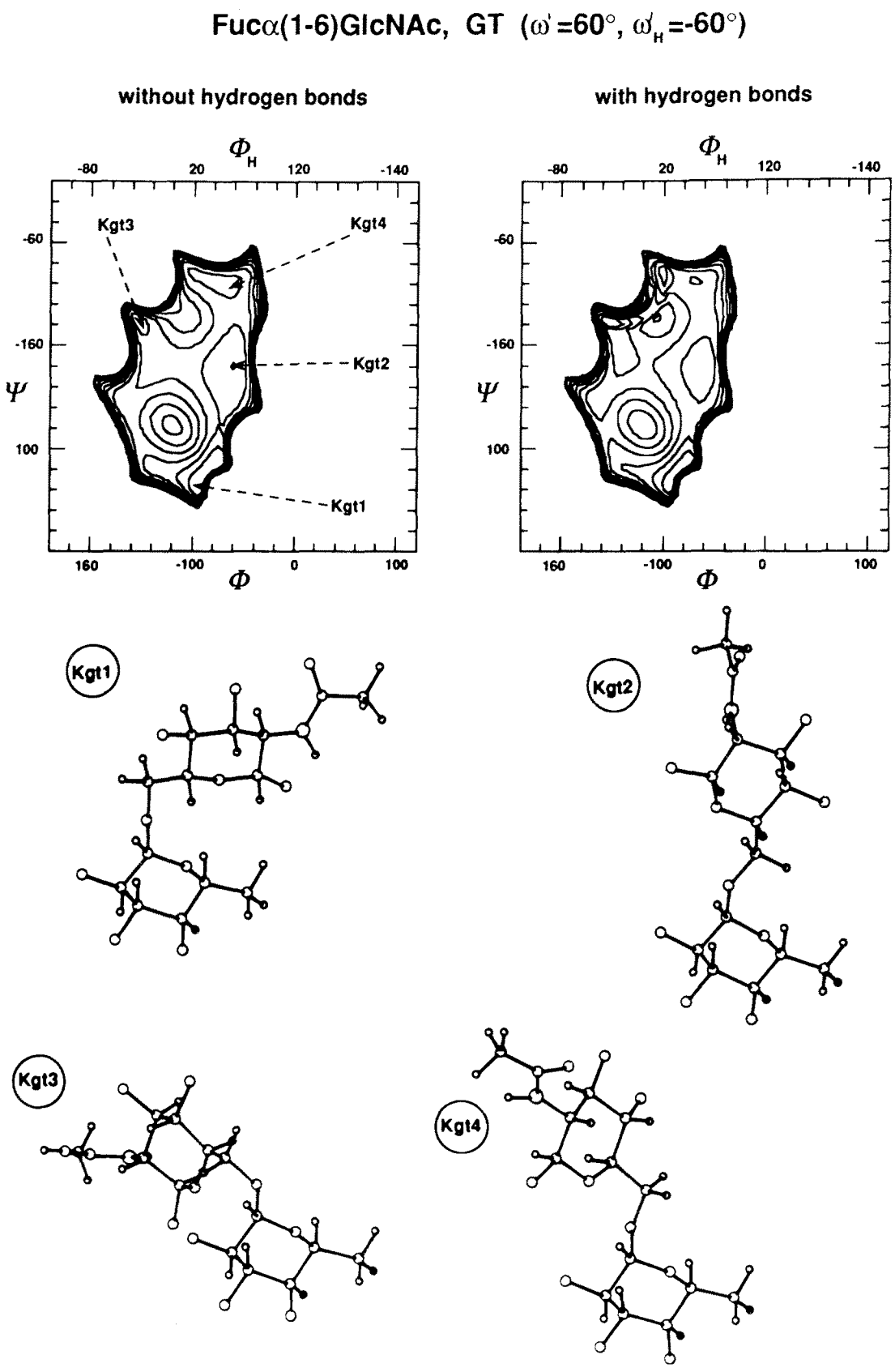

Figure A8. Iso-energy map of the Fucα(1-6)GlcNAc disaccharide computed without (left panel) and with (right panel) the contribution arising from hydrogen bonding. The ω angle at the glycosidic linkage is fixed in the GT orientation. The glycosidic valence angle (τ) has a value of 114.5°. Other details are as in Fig. A1. The drawings represent the energy minima Kgt1 to Kgt4..

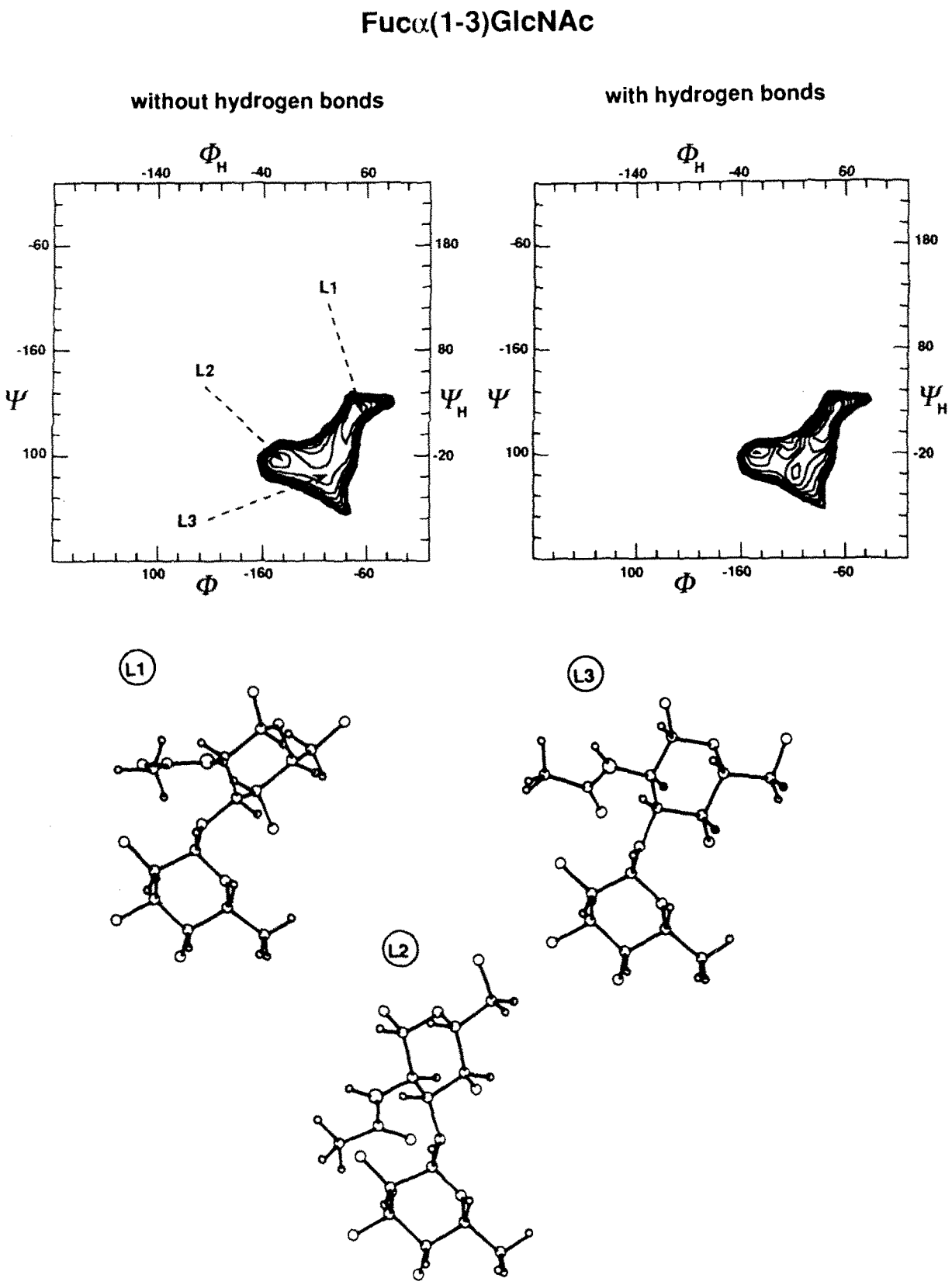

Figure A9. Iso-energy map of the Fucα(1-3)GlcNAc disaccharide computed without (left panel) and with (right panel) the contribution arising from hydrogen bonding. The glycosidic valence angle (τ) is fixed at a value of 115.0°. The *N*-acetylglucosamine hydroxymethyl group is fixed in a GT orientation. Other details are as in Fig. A1. The drawings represent the energy minima L1 to L3.

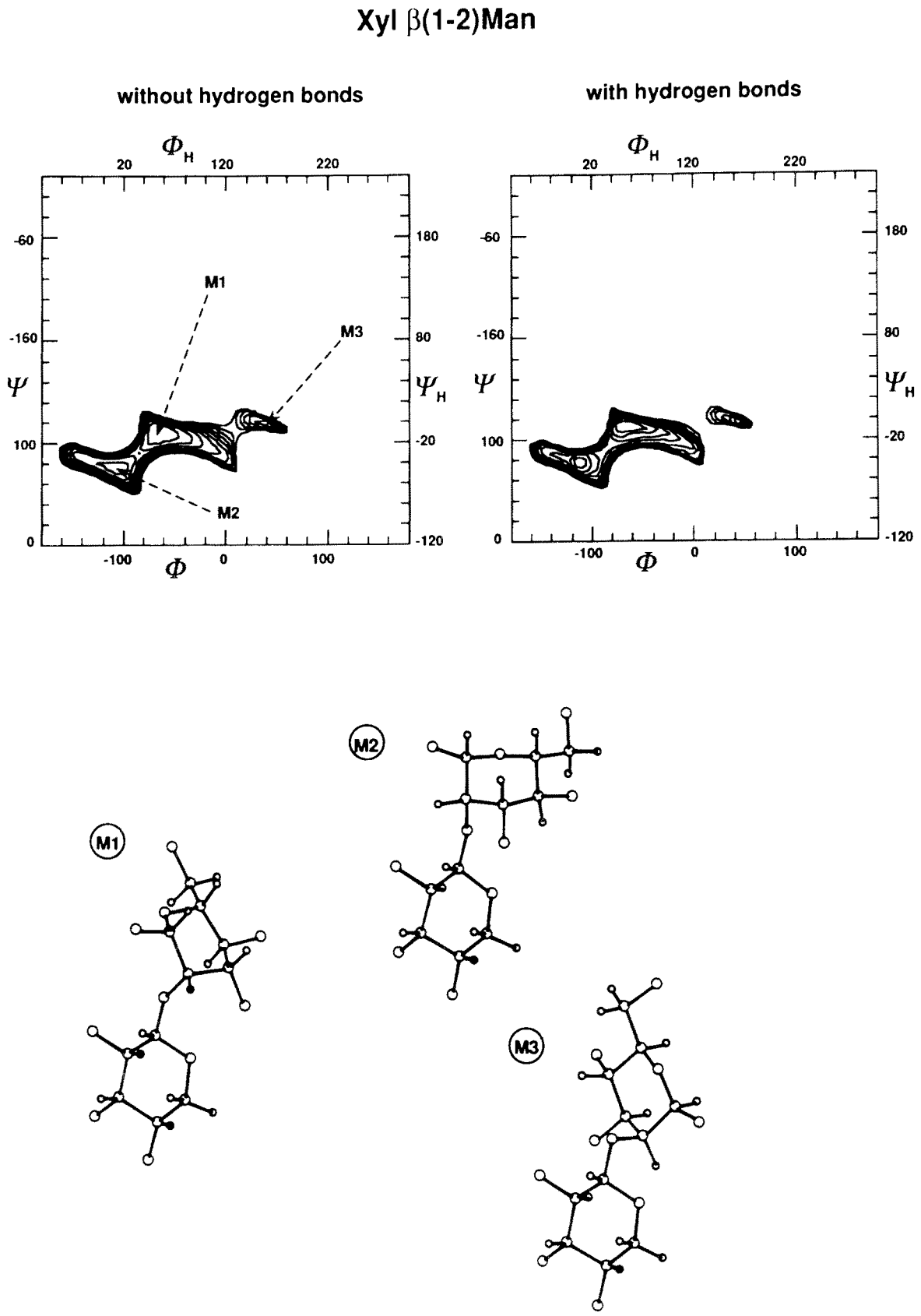

Figure A10. Iso-energy map of the Xylβ(1-2)Man disaccharide computed without (left panel) and with (right panel) the contribution arising from hydrogen bonding. The glycosidic valence angle (τ) is fixed at a value of 116.5°. The mannose hydroxymethyl group is fixed in a GT orientation. Other details are as in Fig. A1. The drawings represent the energy minima M1 to M3.

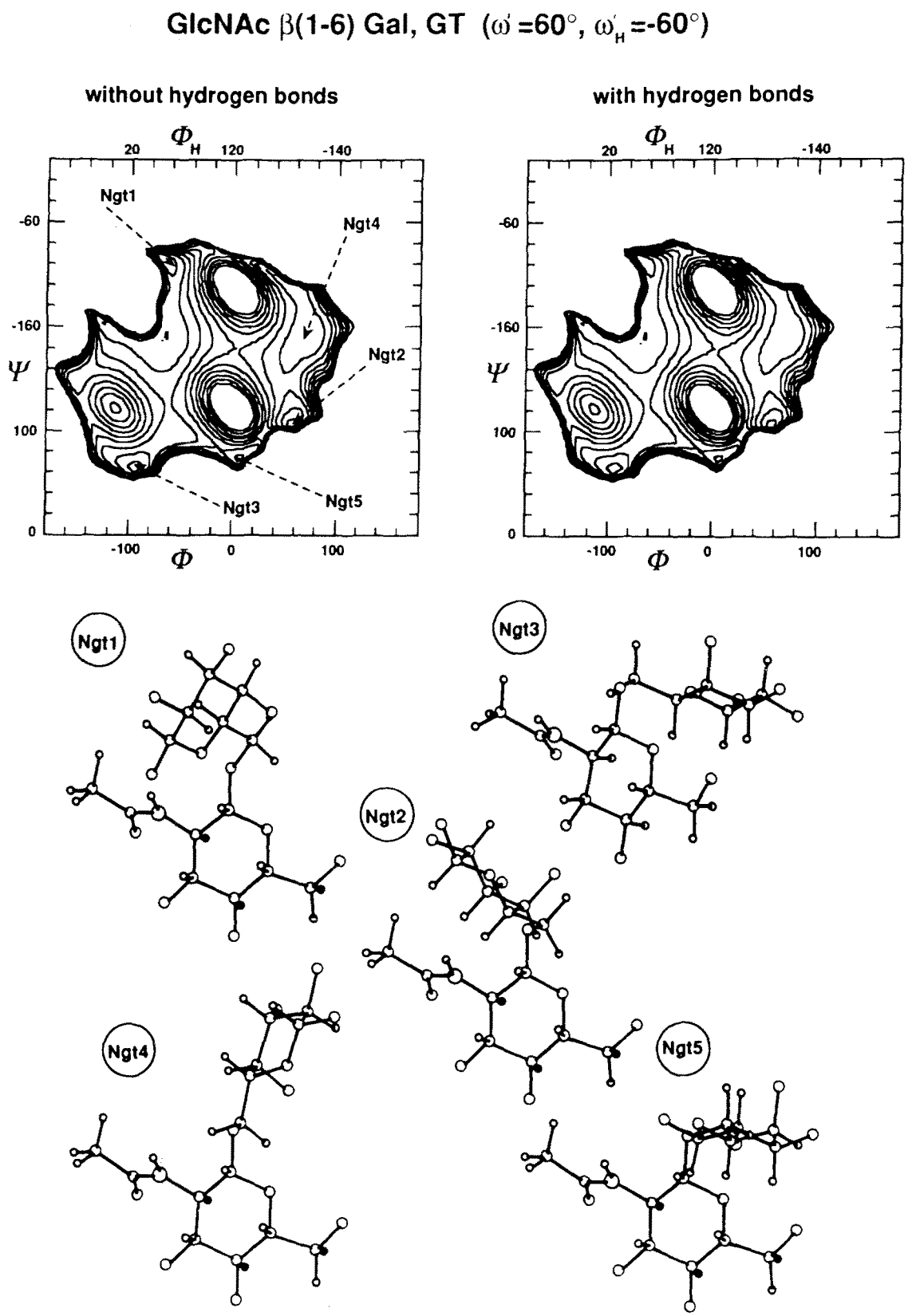

Figure A11. Iso-energy map of the GlcNAcβ(1-6)Gal disaccharide computed without (left panel) and with (right panel) the contribution arising from hydrogen bonding. The ω angle at the glycosidic linkage and the *N*-acetylglucosamine hydroxymethyl group are fixed in the GT orientation. The glycosidic valence angle (τ) has a value of 114.5°. Other details are as in Fig. A1. The drawings represent the energy minima Ngt1 to Ngt5.

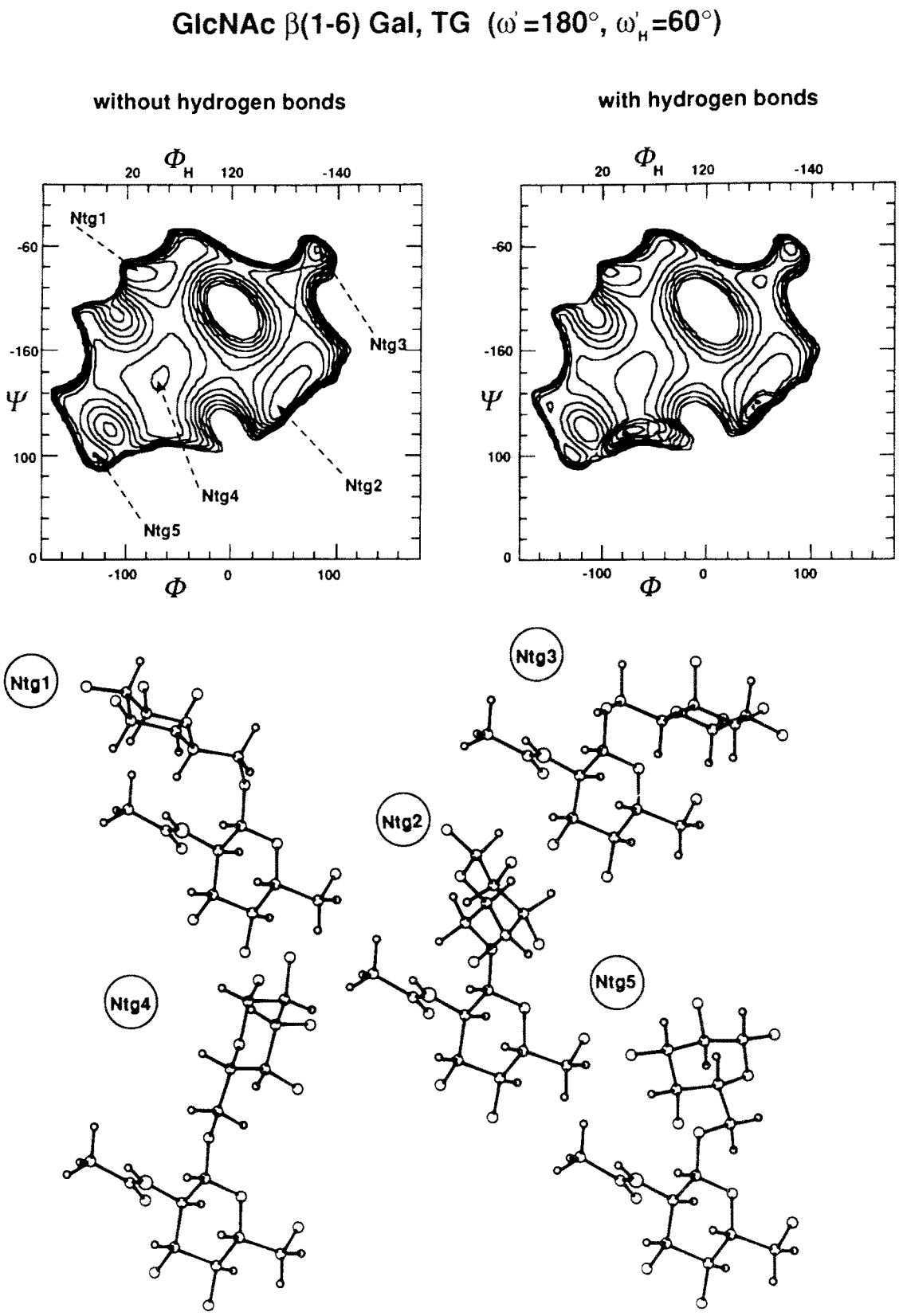

Figure A12. Iso-energy map of the GlcNAc(1-6)Gal disaccharide computed with (left panel) and with (right panel) the contribution arising from hydrogen bonding. The ω angle at the glycosidic linkage is fixed in the TG orientation whereas the *N*-acetylglucosamine hydroxymethyl group has the GT orientation. The glycosidic valence angle (τ) has a value of 114.5°. Other details are as in Fig A1. The drawings represent the energy minima Ntg1 to Ntg5.

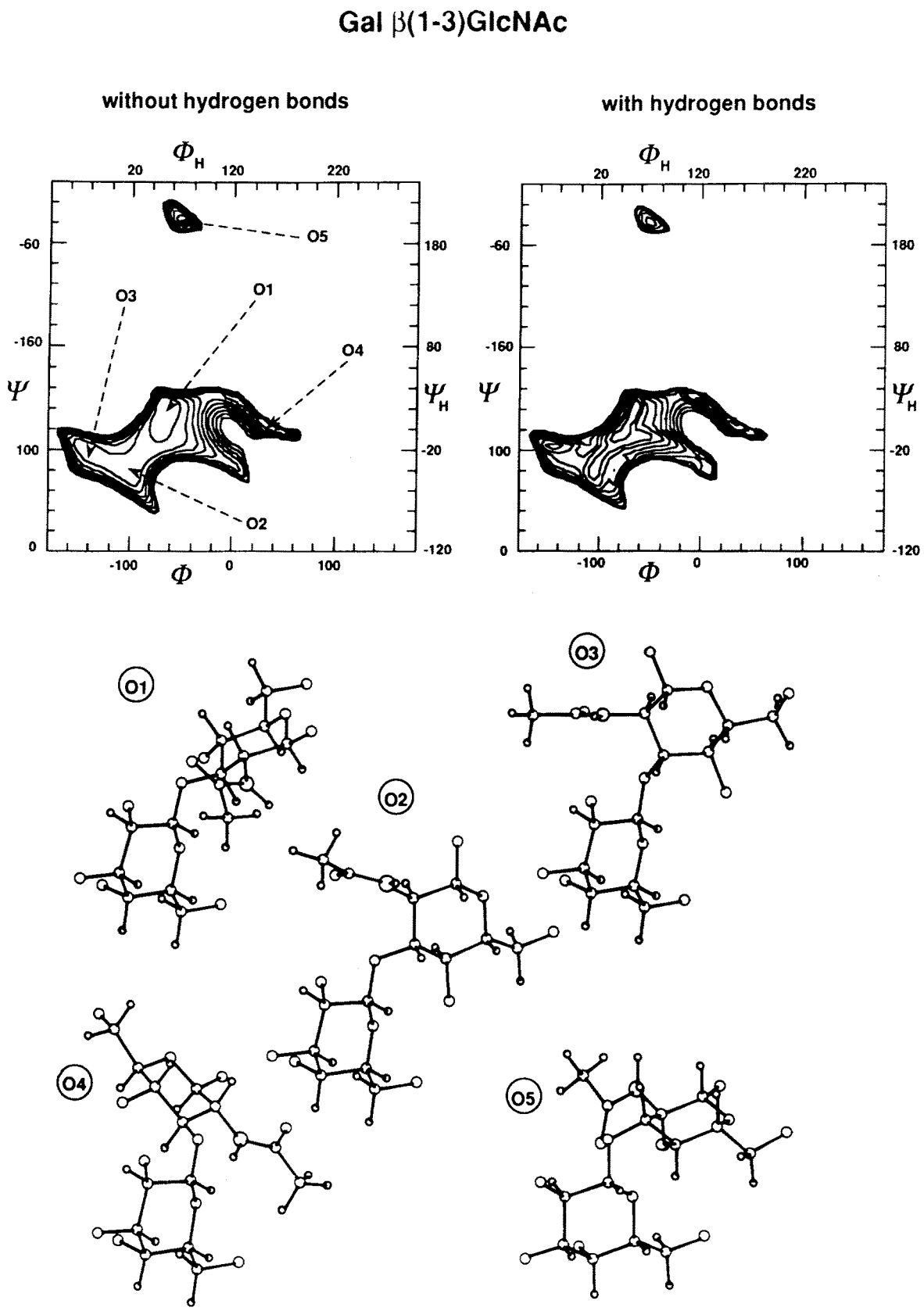

Figure A13. Iso-energy map of the Galβ(1-3)GlcNAc disaccharide computed without (left panel) and with (right panel) the contribution arising from hydrogen bonding. The glycosidic valence angle (τ) is fixed at a value of 116.5°. Both hydroxymethyl groups are fixed in a GT orientation. Other details are as in Fig. A1. The drawings represent the energy minima O1 to O5.

Table A1. Geometrical features, calculated energies (kcal mol^{-1}) and possible hydrogen bonds for the GlcNAcβ(1-6)Gal linkage as calculated by the PFOS program ($\tau = 114.5°$). Torsional angles are given in both the crystallography and the NMR nomenclatures, the two sets being presented respectively without and with parentheses.

Name	Φ, Ψ	(Φ_H, Ψ)	χ, χ'	(χ_H, χ'_H)	*Relative energy*	*Possible hydrogen bond*
Ngt1	−70, −95	(50, −95)	−60, 60	(180, −60)	0.26	
			60, 60	(−60, −60)	0.22	
Ngt2	55, 105	(175, 105)	−60, 60	(180, −60)	0.77	
			60, 60	(−60, −60)	0.79	
Ngt3	−90, 60	(30, 60)	−60, 60	(180, −60)	0.78	
	−95, 65	(25, 65)	60, 60	(−60, −60)	0.89	
Ngt4	55, −115	(175, −115)	−60, 60	(180, −60)	1.93	
	70, −170	(−170, −170)	60, 60	(−60, −60)	2.51	
Ngt5	5, 75	(125, 75)	−60, 60	(180, −60)	2.92	
			60, 60	(−60, −60)	3.01	
Ntg1	−95, −85	(25, −85)	−60, 180	(180, 60)	0.02	
			60, 60	(−60, 60)	0.00	
Ntg2	50, 150	(170, 150)	−60, 180	(180, 60)	1.06	O-7 . . . O-4′
			60, 60	(−60, 60)	1.08	O-7 . . . O-4′
Ntg3	−80, −60	(40, −60)	−60, 180	(180, 60)	1.62	
			60, 60	(−60, 60)	1.78	
Ntg4	−65, 175	(55, 175)	−60, 180	(180, 60)	1.93	O-5 . . . O-4′
	−70, 170	(50, 170)	60, 60	(−60, 60)	1.91	O-5 . . . O-4′
						O-5 . . . O-6′
Ntg5	−130, 100	(−10, 100)	−60, 180	(180, 60)	4.01	
			60, 60	(−60, 60)	3.88	

Table A2. Geometrical features, calculated energies (kcal mol^{-1}) and possible hydrogen bonds for the Galβ(1-3)GlcNAc linkage as calculated by the PFOS program ($\tau = 116.5°$). Torsional angles are given in both the crystallography and the NMR nomenclatures, the two sets being presented respectively without and with parentheses.

Name	Φ, Ψ	(Φ_H, Ψ_H)	χ, χ'	(χ_H, χ'_H)	*Relative energy*	*Possible hydrogen bond*
O1	−65, 140	(55, 20)	60, −60	(−60, 180)	0.00	O-2 . . . O-7′
						O-5 . . . O-4′
			180, −60	(60, 180)	0.08	O-2 . . . O-7′
						O-5 . . . O-4′
			60, 60	(−60, −60)	0.01	O-2 . . . O-7′
						O-5 . . . O-4′
			180, 60	(60, −60)	0.09	O-2 . . . O-7′
						O-5 . . . O-4′
O2	−100, 80	(20, −40)	60, −60	(−60, 180)	1.30	O-5 . . . O-4′
			180, −60	(60, 180)	1.44	O-5 . . . O-4′
			60, 60	(−60, −60)	1.32	O-5 . . . O-4′
			180, 60	(60, −60)	1.45	O-5 . . . O-4′
O3	−145, 100	(−25, −20)	60, −60	(−60, 180)	1.42	O-2 . . . N′
			180, −60	(60, 180)	1.44	O-2 . . . N′
			60, 60	(−60, −60)	1.42	O-2 . . . N′
			180, 60	(60, −60)	1.45	O-2 . . . N′
O4	45, 120	(165, 0)	60, −60	(−60, 180)	2.94	O-2 . . . O-4′
						O-5 . . . N′
	45, 125	(165, 5)	180, −60	(60, 180)	1.46	O-2 . . . O-4′
						O-5 . . . N′
	45, 120	(165, 0)	60, 60	(−60, −60)	2.95	O-2 . . . O-4′
						O-5 . . . N′
	45, 125	(165, 5)	180, 60	(60, −60)	1.47	O-2 . . . O-4′
						O-5 . . . N′
O5	−50, −35	(70, −155)	60, −60	(−60, 180)	3.27	
			180, −60	(60, 180)	3.67	
			60, 60	(−60, −60)	3.44	
			180, 60	(60, −60)	3.77	